EXTRUSION OF LOW DENSITY POLYETHYLENE TUBULAR FILM

BY

BAHA ELDIN SIDDIG

A Thesis submitted for the award of the Degree of Master of Science of the Loughborough University of Technology.

1974

Supervisor: D.E. Marshall, Ph.D.
Institute of Polymer Technology

ACKNOWLEDGEMENTS

I wish to express my gratitude to Dr. D.E. Marshall, Loughborough University of Technology, for suggesting the problem and guidance throughout the work.

My thanks are also due to Professor A.W. Birley, Director of the Institute of Polymer Technology, for his encouragement and for giving many facilities.

My gratitude is due to members of the Institute for their help.

My special thanks go to the British Council for the financial support.

Acknowledgement is also made to I.C.I. Plastics Division, for giving the raw materials for the work.

I certify that this work has not been submitted to this or

any other institution for consideration of a degree

SUMMARY

Melt capillary flow has been employed to characterise some low density polyethylene grades, differing in degree of an incorporated slip agent (Olemide Commercial).

The same grades were processed into blown film under different extrusion conditions by varying screw speed, blow-up ratio and haul-off rate.

The rheological properties affected by the slip agent were, namely, the melt viscosity and the critical shear-rate, after which fracture (turbulence) of the given extrudate occurred.

Ease of draw-down property was found to be lower for the low slip grades and increased significantly with increasing degree of slip.

(ASTM) and (B.S.) methods were used to test the mechanical properties of the films produced from the film-blowing process under the same above extrusion variables. The effect of these variables on tensile, tear and impact strengths of each grade were analysed. Orientation of the molecular structure, during its passage through the die and immediately after extrusion, as a result of longitudinal or transverse direction drawing strongly affected these properties.

Increasing the extrusion variables, generally, resulted in a balanced orientation in both machine and transverse directions (balanced film) and an optimum blow-up ratio was found for a film of balanced strength properties.

An attempt was made to correlate characteristics of flow of the different polyethylenes with the above extrusion variables and, hence, with the mechanical properties of the consequent films.

CONTENTS

Section 3

Results

3.1 Flow Properties Investigations

3.1.1 Shear-stress Shear-rate dependence

3.1.2 Shear-rate Dependence of Melt Viscosities

3.1.3 Critical Shear-rate

3.1.4 Apparent Energy of Activation

3.2 Effect of Extrusion conditions on Mechanical Properties of the low Density Polyethylene Films

3.2.1 Haul-off Rate

3.2.2 Effect of Blow-up Ratio

3.2.3 Effect of screw speed

Section 4

Discussion of the Results and Conclusion

4.1 Flow of the Low Density Polyethylene Grades

4.2 Activation Energy

4.3 The Extrusion Process of Low Density Polyethylene Film

4.3.1 Orientationof Blown Film

4.3.2 Effect of Rheological Properties on the Mechanical Properties of the Film

4.3.3 Effect of Extrusion Conditions

(i) Tensile and Impact Strength

(ii) Elongation-Tear Relationship

4.3.4 Conditions of Balanced Film

4.3.5 Birefringence

4.4 Conclusions

Section 1 : Introduction and Background

1-1 Introduction :-

Polyethylene film has come to the fore in recent years as a replacement material for paper in the retail bag and certain other markets, where greaseproof and waterproof qualities are particularly desirable. The production of various types of packaging film, from the heavy duty sack to the high-clarity textile display material, forms the largest outlet for low density polyethylene.

Some years ago a great deal of discussion took place concerning the properties of the ideal film. As the range of materials to be packaged broadened, the number of specific requirements grew enormously, and one hopes for as many of the desirable properties in a single film as is possible. Amongst the diverse requirements for the end product are the following properties:

(a) Good optical properties.

(b) Excellent mechanical properties (high impact, tensile and tear strengths.

(c) Ability and ease to draw down to a thin accurate gauge film.

Since film processing involves working the polyethylene grade in the melt, semi melt and solid states, its rheological properties play a very important part in defining the processing characteristics and final product properties.

Although the polymer selection and film processing parameters have been investigated in detail, particularly in the case of the retail bag market, where greater demands are made in film properties, very few

attempts have been made to correlate rheological properties with processing conditions. A basic understanding of film technology requires some knowledge of rheological properties in order to understand the fabrication of film.

Many aspects have to be taken into account by the polymer manufacturer in designing a film grade. The general specification for a packaging film can be outlined in terms of physical and chemical properties, grouped functionally in relation to uses. Each application represents a compromise of requirements. As a result, there has been a growing use of additives to give the desired characteristics of the final film, but, at the same time, they can affect processing behaviour and create new compromise.

One of the most important additives to enhance the film properties is the slip agent or lubricant. Polyethylene film must have a good slip from the standpoint of packaging machine operability and easy separation of sheets and fabricated bags, so that the finished product might not be capable of stacking without undue slippage. This is particularly important as processing and packaging machine speeds are increased and new methods have to be sought to regulate film surface properties for optimum machine performance.

Friction of a 'poor slip' film is reduced by applying a lubricant to the film surfaces. In commercial practice these lubricants are mostly derivatives of long-chain fatty compounds.

This work involves study of the rheological properties and the effect of some extrusion conditions on the mechanical properties of low density polyethylene tubular film.

The work may be divided into three main parts:-

(a) Rheology : which involved a study of the flow behaviour of the materials investigated at different conditions of temperature and shear-rates.

(b) Processing of the materials into blown film under different extrusion conditions.

(c) Testing of the film mechanical properties; this involved testing of:

(i) Impact strength

(ii) Tensile strength

(iii) Tear propagation

(iv) Degree of orientation.

1.2 Rheological Properties of Polymer Melts

Flow of polymer melts occurs when plastic materials are processed by extrusion, moulding and calendering techniques. Therefore, it has become very important to study the flow properties of the polymers in order to continue to make progress in polymer processing techniques, and allow to understand processing faults and defects which are of rheological origin, and hence, try to select the best suitable polymer or polymer compound for a given set of circumstances.

(i) Newtonian Fluid (Ideal Fluid):

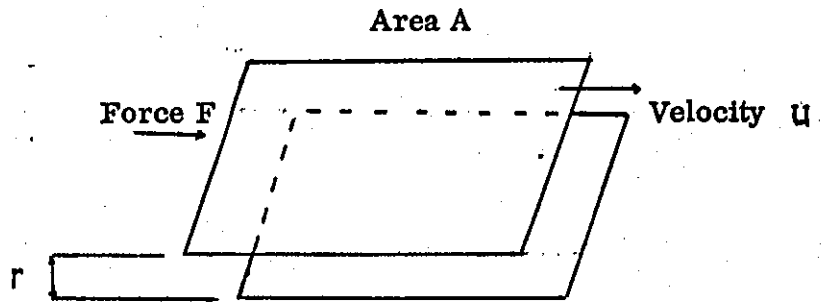

Fig. 1.1

Figure 1.1 illustrates the behaviour of an ideal fluid under the influence of a shearing stress (τ) = F/A. The fluid fills the space between the two parallel plates of area A. On imposition of a force F, the upper plate will move relative to another one at a constant velocity (u) as long as the force remains constant. The fluid exhibits no tendency to return to its original shape when the shearing stress is finally removed. Since the shearing force is transmitted uniformly through the liquid to the lower plate, each layer of the fluid within the space of height (r) will slip relative to the next, setting up a uniform change in velocity with distance. Mathematically, the relationship between this shearing stress and the

resulting change in velocity may be given by either of two equations, since $\frac{u}{r}$ is constant (hence = $\frac{du}{dr}$) :

$$\tau = F/A = \mu \cdot \frac{u}{r} \qquad (1)$$

$$\tau = \mu \cdot \frac{du}{dr} \qquad (2)$$

where:

$\frac{du}{dr}$ = velocity gradient or shearing rate of the fluid,

μ = coefficient of viscosity of the fluid.

In case of the ideal Newtonian fluid, the strain progresses uniformly with time. If in time d t the upper plate has travelled a distance dL, Then the differential strain ($d\gamma$) is given by:

$$d\gamma = \frac{dL}{r} = \frac{U}{r}\, dt \qquad (3)$$

or $$\frac{d\gamma}{dt} = \frac{u}{r} = \frac{du}{dr} = \frac{\tau}{\mu}$$

or $$\tau = \mu \frac{d\gamma}{dt} = \mu \cdot \dot{\gamma} \qquad (4)$$

For an ideal Newtonian fluid, where:

$\dot{\gamma}$ = the shear-rate or rate of shear strain. Newton's equation implies that viscosity at any given temperature is iindependent of the shear-stress and shear-rate. Fluids which obey the above relationship are known as Newtonian fluids.

Taking logarithms of the equation describing Newtonian behaviour:

$$\log \tau = \log \left(\mu \cdot \frac{du}{dr}\right)$$

$$\log \tau = \log \frac{du}{dr} + \log \mu = \log \dot{\gamma} + \log \mu \qquad (5)$$

Thus, the shear-stress shear-rate relationship of a Newtonian fluid becomes

a straight line with a slope of unity on logarithmic co-ordinates. The degree of non-Newtonian behaviour is represented by the amount by which the slope of the log flow curve for a given non-Newtonian fluid differs from unity.

(ii) Non-Newtonian Fluid :

Many real materials, particularly polymer melts do not, however, exhibit the simple characteristic of a Newtonian fluid. For plastic melts, such as low density polyethylene, Newtonian behaviour is detected only at very low stresses well below the range of interest in processing. At higher stresses polymer melts exhibit what is known as pseudoplastic behaviour. That is, the shear-rate increases much more than proportionally with increasing shear stress.

Skelland has summarised the equations which have been proposed to describe pseudoplastic behaviour. Unfortunately, the mathematics used in solving these equations are difficult and rarely justified. For many polymer melts the flow curves approach linearity when plotted in logarithmic form, particularly over limited ranges of shear stress. This linearity, where it exists, implies a power-type relationship between shear stress and shear rate, and this relationship is known as the "Power Law", or Ostwald-de-Waele equation which states that:

$$\tau = k \left(\dot{\gamma} \right)^n \qquad (6)$$

Where K is known as the consistency, and n the degree of non-Newtonian behaviour, or the power law exponent. In logarithmic form equation (3) may be written:

$$\log \tau = \log K + n \log \dot{\gamma} \qquad (7)$$

Thus, equation (6) is represented by a straight line of slope equal to the power law exponent (n).

The apparent viscosity (μ_a) is defined as the quotient of the shear stress divided by the shear rate or,

$$\mu_a = \tau/\dot{\gamma}$$

Equation (6) may be written in terms of the apparent viscosity as:-

$$\mu_a = \eta = K(\dot{\gamma})^{n-1} \qquad (9)$$

Therefore, the viscosity, μ, will also exhibit a power law-type dependence on shear rate according to the equation:-

$$\frac{\eta}{\eta_o} = \left(\frac{\dot{\gamma}}{\dot{\gamma}_o}\right)^{n-1} \qquad (10)$$

Where η_o term is called the standard state viscosity and is the viscosity calculated at some convenient standard shear rate ($\dot{\gamma}_o$).

(iii) Elastic Properties of Polymer Melts

In polymer melts the chains tend to uncoil as they are sheared. On release of the shearing stresses the polymer molecules will tend to recoil again and be pulled back by restraining forces. The elastic strain present in viscoelastic polymer melts can be seen clearly in the "die swell" of the emerging polymer stream. The swelling ratio, defined as the ratio between the diameters of the melt profile and the die, gives some indication of the magnitude of the elastic properties.

Die swell effects have been investigated by many authors (Benynon and Glyde, Bagley and Clegg). Many theories have been proposed to

explain die swell in polymer melts and its correlation with normal stress and end effects. In capillary flow corrections have to be made for what is known as 'entry effects'. Polymer melts have considerable elasticity and as they approach the small orifice opening from the larger reservoir they resist being deformed into the new constricted flow channel. This entrance deformation consumes considerable energy which results in a drop in pressure at the orifice entrance.

An important phenomenon known as "melt fracture" or 'elastic turbulence' has been observed to occur as the flow rates are increased. In several polymers the flow rate at which such irregularities first appear are very low. This phenomenon therefore severely limits the maximum permissible flow rate which may be used in industrial extrusion operations. Therefore, for any polymer there is a certain critical shear-rate above which the surface of the extrudate becomes rough. Reiner has suggested two possibilities for the cause of roughness in extruded viscoelastic materials:

a) Turbulence after the disappearance of laminar flow at the critical Reynold's number and (b) Structural breakdown by fracture within the polymer melt. The latter type of disturbance is the most commonly accepted in studies of flow properties and has been described by Tordella under the name of melt fracture.

For Newtonian fluids turbulence appears at Reynolds numbers ranging from 2000 to 3000. The criterion for roughness is a critical maximum shear-stress or shear-rate at and above which the extrudate irregularity increases. Tordella suggested that as a result of the slow relaxation times relative to the deformation rates, the stress exceeds the

strength of the melt and a fracture results. In 1963, Benbow and Lamb published details of a number of experiments which indicated that the locus of origin of turbulence was at the die wall. The basic causes of the effect of melt fracture are still in dispute, and hence no recommendations for methods of controlling or reducing the magnitude of the irregularities are yet possible.

Howells and Benbow have found that an increase in temperature causes a large increase in the critical shear-rate but has less effect on the critical shear-stress.

Clegg investigated melt fracture in different polyethylene samples. His work indicated that polymers which show flow irregularity at low output rates are those with comparatively long relaxation times. Clegg's work was con firmed by Bagley, Storey and West who experimented with polyethylene and came to similar conclusions.

(iv) Effect of Temperature on Melt Viscosity

It was pointed out earlier that, for many polymers at temperatures considerably above their glass-transition temperatures, the melt viscosity has been experimentally determined to be an exponential function of the absolute temperature.

Theory developed by Henry Eyring has led to the widespread expression of temperature sensitivity of viscosity in terms of an activation energy. This is defined by the Arrhenius equation:-

$$\mu = Ae^{\Delta E/R_o T} \qquad (11)$$

where:- R_o = universal gas constant

A = constant

ΔE = energy of activation for viscous flow

In non-Newtonian fluids the viscosity depends on the shear-rate ($\dot{\gamma}$) or shear-stress (τ), and therefore, it is necessary to keep either τ or $\dot{\gamma}$ constant in order to isolate the temperature's effect. The viscosity change with temperature at constant τ can be proved mathematically to be different from the viscosity change with temperature at constant $\dot{\gamma}$ as follows:-

The total differential of μ as f (τ, T) is:

$$d\mu = \left(\frac{\partial \mu}{\partial T}\right)_{\tau} dT + \left(\frac{\partial \mu}{\partial \tau}\right)_{T} d\tau$$

If $\dot{\gamma}$ is constant:

$$d\mu = \left(\frac{\partial \mu}{\partial T}\right)_{\tau} dT + \left(\frac{\partial \mu}{\partial \tau}\right)_{T} \left(\frac{\partial \tau}{\partial T}\right)_{\dot{\gamma}} dT$$

or, $$\left(\frac{\partial \mu}{\partial T}\right)_{\dot{\gamma}} = \left(\frac{\partial \mu}{\partial T}\right)_{\tau} + \left(\frac{\partial \mu}{\partial \tau}\right)_{T} \left(\frac{\partial \tau}{\partial T}\right)_{\dot{\gamma}}$$

Rearranging and dividing by $\left(\frac{\partial \mu}{\partial T}\right)_{\dot{\gamma}}$:

$$\frac{\left(\frac{\partial \mu}{\partial T}\right)_{\tau}}{\left(\frac{\partial \mu}{\partial T}\right)_{\dot{\gamma}}} = 1 - \left(\frac{\partial \mu}{\partial \tau}\right)_{T} \left(\frac{\partial \tau}{\partial \mu}\right)_{\dot{\gamma}}$$

Differentation of the basic equation $\tau = \mu \cdot \dot{\gamma}$ with respect to μ at constant $\dot{\gamma}$ gives:

$$\left(\frac{\partial \tau}{\partial \mu}\right)_{\dot{\gamma}} = \dot{\gamma}$$ and this reduces the above equation to:

$$\frac{\left(\frac{\partial \mu}{\partial \tau}\right)_{\tau}}{\left(\frac{\partial \mu}{\partial T}\right)_{\dot{\gamma}}} = 1 - \dot{\gamma} \left(\frac{\partial \mu}{\partial \tau}\right)_{T} \quad (12)$$

In pseudoplastics μ decreases as τ increases and, therefore, $\left(\frac{\partial \mu}{\partial \tau}\right)_{T}$ is -ve and the right-hand side of equation 16 must be > 1.

Therefore, for a pseudoplastic:

$$\left(\frac{\partial \mu}{\partial T}\right)_{\tau} > \left(\frac{\partial \mu}{\partial T}\right)_{\dot{\gamma}}$$

The two μ derivatives become equal when either:

$\frac{\partial \mu}{\partial \tau} = o$ and the fluid is Newtonian in this case, or

$\dot{\gamma} = o$, and this raises the interesting fact observed by many authors that all fluids at zero shear are in fact Newtonians.

Rewriting equation (11) in the logarithm form:-

$$\ln \mu = \ln A + \frac{\Delta E}{R_g T}$$

Plots of $\ln \mu$ versus $\frac{1}{T}$ may be useful to calculate the apparent activation energy (ΔE).

Mendelson has shown that for low density polyethylene the Arrhenius equation applies accurately only if the melt viscosities are compared for equal shear-stresses and that the activation energy varies if shear-rate is taken as the basis for comparison.

Philippoff and Gaskins have investigated in detail the relationship of viscosity with temperature for a set of different polymers and presented an excellent summary of all work at low shear-rates.

1-3 Capillary Flow

The most commonly used method of measuring the flow behaviour of polymer melts is by applying pressure to the melt and thereby forcing it to flow from a reservoir through a short circular tube. It was observed that the output (Q) was proportional to the pressure (ΔP) in case of liquids such as water, and the following equation, which is known as Poiseuille's Law, could be postulated:-

$$Q = \frac{\pi \Delta P R^4}{8 \mu . L} \qquad (13)$$

Where:

R = radius of tube of length L

μ = the coefficient of viscosity

For non-Newtonian fluids the following assumptions have to be made in order to derive quantitative relationships:

(i) Velocity of fluid at the wall is zero (no slip).

(ii) Fluid is time independent.

(iii) Flow pattern is constant.

(iv) Flow is isothermal.

(v) The melt is incompressible.

Consider the balance of forces for flow through a capillary:

$$\tau w \times 2\pi RL = \Delta P \times \pi . R^2$$

where Tw = shear-stress per unit area at the wall of the tube

$2\pi RL$ = area of contact of moving cylinder of liquid along capillary wall,

ΔP = pressure difference at capillary ends,

πR^2 = area over which pressure is exerted.

Therefore $\tau w = \frac{\Delta PR}{2L}$ (14)

Rewriting equation (13) :-

$$Q = \frac{\Pi \Delta P R^4}{8 \mu L}$$

Making μ the subject of this equation:

$$\mu = \frac{\Pi \Delta P R^4}{Q.8L} = \frac{\tau w}{\dot{\gamma} w} \quad \text{(by definition)}$$

$$\frac{\Pi \Delta P R^4}{8QL} = \frac{\Delta P R}{2L \dot{\gamma}_w} \quad \text{(by substitution for } \tau w)$$

$$\therefore \quad \dot{\gamma} w = \frac{4Q}{\Pi R^3} \qquad (15)$$

A functional relation was found between τw and the term $Q/ \Pi R^3$. This relation may be written as:

$$\frac{Q}{\Pi R^3} = \frac{1}{\tau_w{}^3} \int_0^{\tau_w} \tau^2 f(\tau) \, d\tau \qquad (16)$$

Where:

f = the function connecting shear-stress and shear-rate. It can be seen that from equation (16), $\frac{Q}{\Pi R^3}$ depends only on τw and independent of tube size.

A superimposition of flow curves for data obtained from measurements using capillary tubes of different diameters would show absence of both time-dependence and slip at the wall.

Entry Effect in Cappillary Tubes:

A method has been proposed for the elimination of entry effects by using pairs of capillary tubes of equal radii and lengths l_1 and l_2 for which pressures P_1 and P_2 are required, respectively, in the same reservoir to obtain an equal output (Q). By using $l_1 - l_2$ and $P_1 - P_2$ instead of l and P, most of the entry effects can be eliminated.

1-4 Principles of Extrusion

Extrusion is employed in the production of plastic films, pipes, sheet, profiles and coatings on wire, paper and other substrates.

The elements of a typical single-screw extruder are shown in Fig. (1.2). The plastic material is fed from a hopper through the feed throat into the channel of the screw. The screw rotates in a barrel which has a hardened liner. The screw is driven by a motor through a gear reducer and heat is usually applied around the barrel and die. As the plastic granules are conveyed along the screw channel, they are melted. The melt is forced through a breaker plate which supports a screenpack and then flows through the die. The size of single-screw extruders is described by the inside diameter of the barrel. The length-to-diameter ratio (L/D) is an important design specification of an extruder. This ratio is the effective length of the machine (from the rear of the feed hopper to the breaker plate) divided by the nominal diameter (inside diameter of the barrel). For thermoplastic extruders, $(\frac{L}{D})$ ratios normally are between 16:1 and 24:1.

Extruder barrels may be heated electrically, either by resistance or induction heaters, or by means of jackets through which oil or other heat transfer media are circulated.

The screw is the most important component of the extruder. Its function is to convey unplasticated resin from the hopper and deliver it to the die at a uniform rate as a homogeneous melt.

The barrel of the extruder is composed of the following sections:

(i) Feed section : The function of the feed zone is to pick up cold material from the hopper and feed it at a moderate pressure to allow proper functioning of the compression zone. The solids feeding depends largely on the bulk density of the feed material and the coefficient of friction

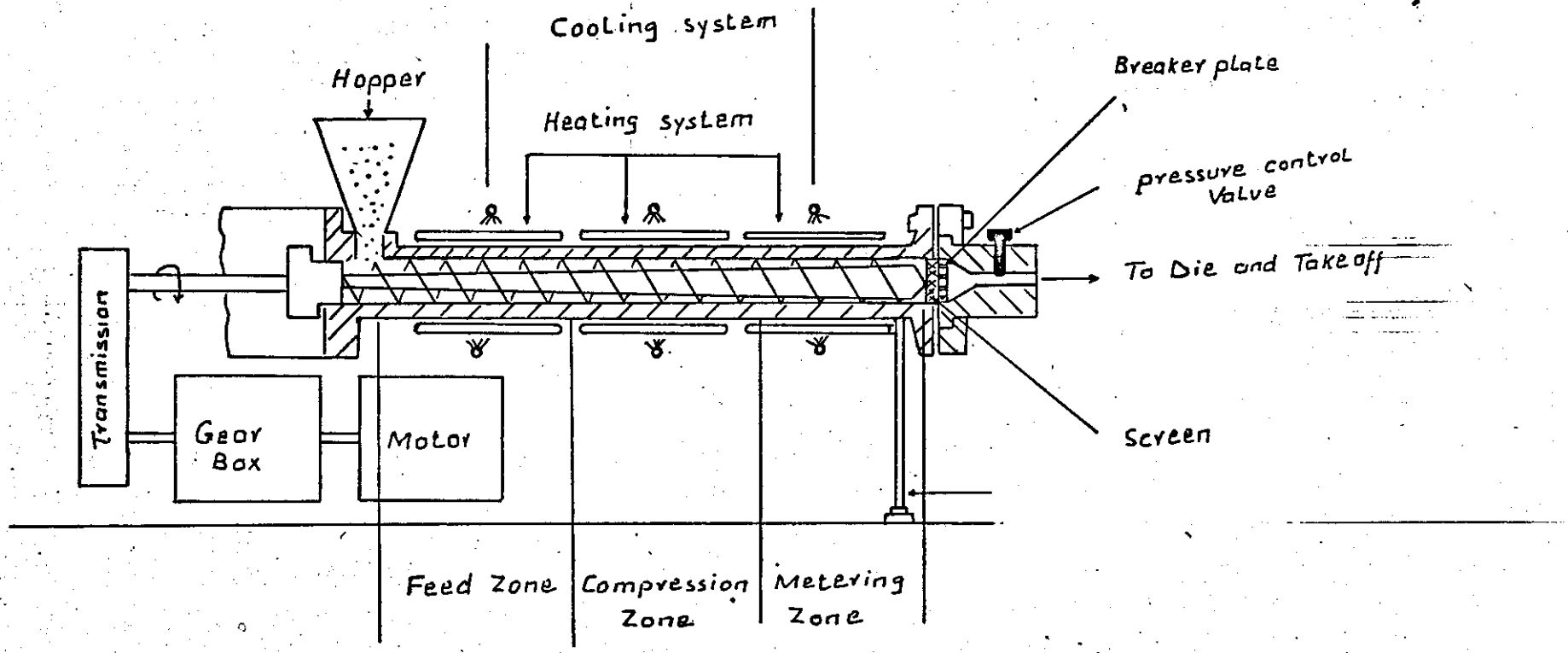

Fig. 12. Dig of a single-screw extruder

between the polymer and the metal parts of the extruder. It has been shown that the most efficient solids feeding occurs when the coefficient is maximised with respect to the barrel and minimized with respect to the screw. Theoretical analysis of the feed zone shows that efficient conveying of the solids is achieved by providing a deep screw channel.

(ii) The Compression (Melting) Zone Section : The compression zone receives the granules from the feed zone and converts it to a dense melt and deliver it at zero pressure to the metering zone. To allow good compression of the material a gradual decrease is made in the channel depth along the zone length.

Heating of the material in the compression zone is achieved by conduction, radiation and internal shearing.

Maddock and Street have provided valuable insight into the mixing and melting processes, particularly in the transition zone.

(iii) The Metering Section : The metering zone of the screw is the section which provides the extruder head with constant pressure and flow rate. The metering section restricts the discharge of the feed and compression sections and thereby causes pressure to be built up at the forward end of the feed section. This pressure contributes to the over-all pressure difference across the metering section and hence influences the pressure flow through the metering section. As the channel is usually more shallow in this zone, the shear rates are higher and the mixing is more intense.

Extruders manufactured with two (twin-screw extruders) or more screws are known as multiple-screw extruders. The multiple-screw extruders may be of an intermeshing or a nonintermeshing type. Those with intermeshing screws tend to operate as positive-displacement pumps

and their output is relatively independent of back pressure. They consume less energy than single-screw machines, and their plasticating capacity is more dependent upon heat transfer from external heaters.

Nonintermeshing screws are usually made to rotate in opposing directions. Twin-screw extruders of this design find application in resin compounding.

1-5 Production of Sheet and Thin Film by Screw Extruder

(i) Production of Sheet

Sheeting is differentiated from film by thickness. Shaped plastics which have a maximum thickness of 0.010 in. are referred to as films. Those having a thickness greater than 0.010 in. are called sheeting.

Sheet is made by forcing thermoplastic through a long horizontal slit. The hot web thus made is carried around polished metal cooling rolls, drawn through rubber pull rolls and is then cut up or rolled as desired. The plastic materials used for this purpose are generally high density polyethylene, P.V.C., high-impact polystyrene and A.B.S. Sheet extrusion grades usually have a high melt viscosity, because die resistance is relatively low and the physical properties are better (high molecular weight).

Thin films are also manufactured by calendering and solvent casting. Chill roll casting of polyethylene has become an established processing technique for the preparation of flat film. Several authors have reported on the relationship between processing variables and film properties of chill cast film and compared them with blown film. Generally, it has been observed that chill cast film will excel in opticals by exhibiting higher gloss and lower haze than will blown film prepared from the same resin.

(ii) Production of Tubular Film :

In the tubular film process a thin tube is extruded and by blowing air through the die head the tube is inflated into a thin bubble. This is cooled by external air, collapsed by nip rolls and wound up either as a tube or slit into flat film. The ratio of the bubble diameter to the die diameter is known as the blow-up ratio (B.U.R.), and the distance between the die and the frost line, where the extrudate becomes solidified, is known as the freeze-line distance. The reduction in thickness of the extruded film

is obtained by expanding the extrudate diameter as well as by differential speeds in the machine direction. The die diameters usually range from 3 to 6 times the diameter of the extruder screw, and they are end or side-fed with the tubing normally extruded upward, or, in some cases downward and horizontal.

In order to maintain expansion of the bubble, it is necessary that expansion should be started as the molten polymer leaves the die lip before it is cooled. This comprises the critical zone in which the film is transformed from a fluid to an oriented, cooled plastic film. Film properties (mechanical and optical) are developed in this zone.

Dies for tubular extrusion are either center-fed or side-fed dies. Center-fed dies are preferable for uniform flow which yields uniform thickness. Side-fed dies are generally employed for production of films having large diameters (12 in. and over). Film dies are usually heated by bands or similar resistance heaters.

Cooling of the extrudate is maintained by employment of air rings which are built in such a way so that the gap through which the air flows can be varied in width, thus varying velocity.

1-6 Properties of Thin Film :

The general specifications of a packaging film can be outlined in terms of physical properties according to requirements. Generally the following characteristics are the most important for a packaging film:

(i) Appearance : A polymer film should be transparent and free from haze or particles and must have a high gloss.

(ii) Printability : A film should be printable by standard techniques at modern press speeds, and therefore, its surface should not be inert to wetting and solvents.

(iii) High-impact : A high impact film is very important especially for goods which are to be shipped and exposed to vibration and sudden shock. A film with high impact strength is capable of distributing stresses without rupture.

(iv) Tear and Tensile Properties : A packaging film should possess a high tensile strength and high tear resistance (tear initiation and tear propagation) to be able to resist shocks during handling operations.

(v) Handling Properties : Handling characteristics of a film are most affected by blocking, coefficient of friction (slip), and static electricity buildup. These properties control the rate at which the film can be processed. A packaging film should slip easily during fabrication and must not develop static electricity which might cause fairly high shocks to operators and delay production.

Moreover, a film must also resist degradation which may be caused by direct exposure to light and sun rays. Good handling characteristics can be maintained by the incorporation of additives to the base polymer (slip and antistatic agents and antioxidants).

1-7 Effect of the Processing Conditions

It is well known that the properties of the film are strongly dependent on the processing conditions as well as the polymer used. It has been shown that the higher the density the lower the flexibility, the greater the brittleness and the less susceptability to blocking.

In recent years there has been extensive investigations into the effect of processing conditions on both mechanical and optical properties of low density polyethylene film. It has been shown that film properties are largely dependent on extrusion variables such as blow-up ratio, melt temperature, draw down speed, extrusion rate, cooling rate and freeze-line distance. These extrusion variables can all be adjusted to give optimum properties.

Huck and Clegg have given an excellent summary of these effects, which can be summarised as follows:-

(i) Optical Properties :

Factors which cause light scattering are mainly:

(a) Surface irregularities due to melt flow.

(b) Crystallization, and

(c) Melt drawing.

When extruding low density polyethylene, the elastic nature of the melt causes a complex pattern of surface irregularities to form as the melt leaves the die. These are influenced by the nature of the resin, shear-rate (output), melt temperature and die profile.

The second major cause of surface irregularities comes from the growth of crystallites near the surface of the film, which distorts the surface.

Extrusion variables greatly affect light scattering. Increased freeze-line distance (F.L.D.) decreases haze. Increasing extruder temperature improves optical properties because the melt is less elastic, so produces fewer extrusion defects. Increasing output rate increases the extrusion defects, but decreases crystallization irregularities because of the increased rate of cooling.;

(ii) Mechanical Properties:

The impact strength is increased by increasing blow ratio. Under some conditions impact strength increases with output rate. The effect of freeze-line distance is also detected. The bubble shape, which changes with output and freeze-line distance shows the order in which transverse and longitudinal draw occurs, and this affects the amount of each frozen orientation into the film.

Tensile strength gives no indication of serviceability, but elongation is broadly related to impact and tear.

Polymer melt flow behaviour is indicated by swelling ratio (melt elasticity). Temperature gradient between die and freeze-line is influenced by cooling arrangements. Impact strength increased as air ring was moved from die to a position $3\frac{1}{2}$ inches above the die.

These concepts have shown to be applicable not only to blown film but also to cast and water bath film.

1-8 Orientation in Polyethylene Film

One of the most important characteristics of polymers is the ease with which the molecules and crystallites orient when the polymer is deformed. Polyethylene is the most extensively studied polymer with regard to orientation. When a polymer is oriented many of its properties may be modified or the polymer may become anisotropic with respect to certain properties. Polyethylene is a polycrystalline polymer in that the polymer molecules are assumed to be arranged in a crystalline and non-crystalline phases. Deformation of the polyethylene film results in an orientation of both crystalline and amorphous regions with respect to the deformation direction.

(i) Theory of Stress-Induced Orientation:

In stress-induced orientation polymer chains are displaced by hot stretching or drawing from a completely random entanglement to a more orderly arrangement parallel to the direction of stress. When the chains have become straightened, mutual attraction between the chains is increased as they are now in a position to exert the greatest possible secondary valance forces on each other. Since more secondary valence bonds must now be broken, slippage is reduced in the direction of alignment. Because of that and the unfolding of the polymer chains, an increase in tensile strength and elastic modulus results. If stress is applied to a hot mass of randomly coiled and entangled chains, the polymer chains disentangle and straighten and alsoslip past one another. There are three components to this:- E_1 the instantaneous elastic deformation caused by valence-angle deformation or bond stretching, which is completely recoverable when the stress is removed. E_2, the molecular alignment deformation caused by uncoiling, which results in a more linear molecular arrangement parallel

to the surface and which is frozen into the structure when the material is cooled. E_3, the non-recoverable viscous flow caused by molecules sliding past one another. E_2 is the orienting component or the major component of the stretching process.

When a film is rapidly stretched at a temp. slightly above its glass transition temperature (Tg), E_1 deforms instantaneously, then begins to retract as E_2 deforms. If the response time of E_3 is greater than that of E_2 under the applied stress, then at some time t_1, E_2 is relatively large and E_3 still small. If the material is rapidly quenched at this point, the alignment deformation E_2 is frozen into the structure. Stretching is thus a dynamic process in which orientation and return to random coil (relaxation) occur simultaneously.

(ii) Biaxial Orientation :

There are two types of orientation :

(a) Uniaxial orientation which takes place during the drawing of a filament where the polymer chains are aligned in one direction only.

(b) Biaxial Orientation which occurs when a film is drawn in more than one direction, commonly at two axis at right angles to one another. The first biaxial orientation process was developed in Germany about 1935. Balance in biaxial orientation is the result of the relative degrees of stretching in different directions during the orientation process. For packaging it is always desirable to have a film as nearly balanced as possible. As the degree of orientation in a biaxially oriented film becomes greater in one direction than in another, values of properties in the one direction increase at the expense of those in the other direction.

1-9 Deformation of Polyethylene Film

The number and nature of the phases present in the polymer are still subjects of active investigation and speculation. It is agreed that the molecules will be ordered differently in each phase and the observed properties of the polymer will be a combination of the individual properties of the molecules in each phase. The first two-phase model of the structure of a polycrystalline polymer was the fringed micelle model, which assumes that the polymer is composed of crystalline and amorphous regions. Some portions of a long molecule lie in the crystalline regions, while other portions wander randomly between the crystallites and contribute to the amorphous region. It is assumed that sections of molecules become arranged in an ordered array and crystallize to form an intermolecular crystal. There is growing evidence that the crystallites in the polymer may also be in the form of chain-folded, single crystals. The individual single crystal lamellae are believed to be connected to each other through tie molecules which will make them respond co-operatively to a deformation. Keller obtained electron photomicrographs of highly oriented polyethylene fibres in which the observed lamella-like structures whose chain axis is oriented in the fiber axis direction, whereas the long axis of the lamella was perpendicular to the fiber axis direction. Kiho, Peterlin and Geil have demonstrated that twinning and phase changes occur when single crystals of polyethylene are deformed and suggested that molecular tilting and slip which is parallel to the chain axis contribute to the deformation mechanism. Hansen and Rusnick proposed that the controlling mechanism and the cold drawing of polymers is one of crystallographic slip. It can be concluded that the nature of the structure of the crystallites in deformed polymers is uncertain, but that there is an increasing inclination towards

the chain-folded single crystal lamella model. Until now, the two-phase model is the most useful model for the interpretation of the deformation behaviour of films. The observed properties of the polycrystalline polymer will be a result of the mixing of the two phases, the crystalline and the amorphous phases.

1-10 Technique of Measuring Mechanical Properties

(i) Impact Strength

The purpose of the impact test for polyethylene film is to determine the resistance of the film to failure under conditions of high velocity impact.

The falling dart test has taken several forms in regard to the manner of measuring the impact strength of the test specimen. The method adopted by ASTM Committee D-20 on Plastics, ASTM method D1790 (27, 28), has found a wide application. In this test the dart is dropped from a constant height, but the weight of the dart is increased in equal increments from the minimum just light enough not to rupture any test specimens to a maximum just heavy enough to rupture all of the test specimens. Impact failure weight is the weight at which half of the test specimens fail.

In some instances the combination of weight of the dart and height of drop is selected to insure that the test specimens will always be ruptured.

(ii) Tear Strength

The most common tear tests consist of measuring the force required to continue a tear rather than the force required to initiate the tear. The Elmendorf tear test, developed in the 1920's, measures the average force required to propagate a tear through a specified length. Several variations have been developed which measure the propagation tear resistance on one of the more sensitive tensile testing instruments.

(iii) Tensile Strength

Tensile strength is the maximum tensile stress which a material can sustain. It is calculated from the maximum load during a tension test, and the original cross-sectional area of the test specimen. The speed of

testing, type of sample grips used and the manner of measuring the extension must be considered. The specimen is usually gripped at its widened ends and mounted in the tensile testing machine in axial alignment with the direction of pull. It is then loaded by separating the grips at a constant rate until it breaks. The tensile strength is calculated from the load at break and the original area of cross-section.

The elongation at break is expressed as a percentage of the original distance between the reference lines.

The initial grip separation depends on the material being tested. For materials having a total elongation at break of 100% or more the ASTM Method D882 recommends at least 2 in. The speed of testing depends on the type of instrument being used.

(iv) Degree of Orientation

A number of methods are useful in obtaining information on Orientation, of which the following are the most commonly known:

(a) X-Ray Diffraction

By means of X-ray diffraction methods it is possible to obtain detailed information on the crystalline component of a polymer. For a preferentially oriented sample, the intensity around the cone of diffraction will depend on the position of the sample relative to the incident beam. By using some form of pole figure devices the intensity can be obtained for a set of diffracting crystal planes while the sample position is varied systematically.

(b) Dichroism :

In the absorption spectra of oriented solids measured with polarized radiation, the absorption of certain bands may be dependent on the direction of the electric vector. This phenomenon is known as dichroism and is used to obtain orientation and structural information about polymers.

(c) Birefringence :

Birefringence is a measure of the total molecular orientation of a system. It is used in many industrial film plants as a measure of the average orientation of the sample. Birefringence is defined as the difference in the principal refractive index parallel (n11) and perpendicular (n⊥) to the stretch direction. As velocity of light is in the medium is related to the polarizability of the chains, birefringence is a function of contributions from the polarizabilities of all of the molecular units of the sample. The velocity of light in the crystalline region will be different from that in the amorphous region. Tobin and Carrano came to a conclusion that the amorphous material shows only slight orientation even at very high crystallite orientations. Since the molecules are optically anisotropic there is a difference in the principal polarizability parallel and perpendicular to the chain axis. For an unoriented sample the birefringence $\Delta\Pi$ is given by:-

$$\Delta\Pi = n_{//} - n_{\perp} = 0$$

In the past few years several quantitative and qualitative studies of the orientation in polyethylene filmsamples have been made. D.R. Holmes and R.P. Palmer proposed a crystallite orientation similar to that first observed by Nancarrow and Horsley in relaxed drawn filaments, the a axes of the crystallites were stated to be preferentially oriented parallel to the extrusion or machine direction, and the b and c crystallite axes were

randomly arranged in the plane perpendicular to the extrusion direction. From X-ray and optical investigations they showed that the orientation in the films is cylindrically symetrical about the machine direction. Depending on the extrusion conditions the angle made by the chain axes of the crystallites may vary. The measured birefringence is influenced both by the average value of the angle and by the dispersion or distribution of orientation about this value. Clegg and Huck showed a relationship between Birefringence, blow-up ratio and impact strength. From a plot of birefringence against blow-up ratio they showed that birefringence passed through a minimum and then a maximum.

SECTION 2

Experimental Method

Introduction

This section covers the materials used and the mixing procedure of the polyethylene granules and the incorporated additives. A short summary is also included of the following:

(i) Flow equipment and method of investigating flow properties of the polyethylene grades.

(ii) The Extruder used for the film blow process.

(iii) The physical testing methods of the polyethylene film. The work involved the incorporation of an antioxidant, an antistatic and a slip agents.

The experimental work carried out can be divided into four parts:

(1) Preparation of raw material.

(2) Flow properties investigations.

(3) Processing variables investigations of the film-blow process.

(4) Testing of the mechanical properties of the final film.

2.1 Preparation of Raw Material :

Investigations carried out involved working with the following low density polyethylene grades:-

a) Two standard low density polyethylene grades for tubular film production namely:-

XJF/46/41 - Medium slip

XJF/46/63 - High slip

b) Four low density polyethylene grades prepared by incorporating with the base polymer constant quantities of an antistatic agent and an antioxidant and varying amounts of a slip agent. These are summarized in the following table:-

Table 2.1

Base Polymer	Polymer Grade	Additives p · p · m		
		Antistatic agent (Ethomeen T12)	Antioxidant (Topanol OC)	Slip Agent Armid O)
Q1388	MS/5 (Low slip)	100	500	50
	MS/25 (Medium-low slip)	100	500	250
	MS/50 (Medium slip)	100	500	500
	MS/100 (High slip)	100	500	1000

The slip agent 'Armid 0' was obtained from "Armour Hess Chemicals". Other materials were obtained from I.C.I., Plastics Division.

The following table shows main characteristics of the slip agent (Armid O)

Table 2.2

Armid o (Olemide commercial)	Amide	Melting point	Moisture	Flash	
	90% (min)	68°C	0.5	207°C	
	Chain				
	C14	C15	C16	C17	C18	Others
	4.5	0.5	9.5	1.0	79.0	5.5

Blending of the Polymer grades:

Blending of the additives and polyethylene granules was carried out on a two-roll mill. The mill was loaded first with half the polyethylene, then the additives, then the remainder of the polyethylene. The rolls were rotated at 40 rev./min. for about 15 minutes and controlled at a temperature of 135°C. Portions of polyethylene sheet were repeatedly removed from the sides using a doctor knife and returned to the nip of the mill to achieve homogeneity.

Dry sheets of the polyethylene containing the additives were taken and milled in a granulator to approximately the same previous size of granules.

2-2 Flow Properties Investigations

Flow Properties studies were carried out using a Davenport Extrusion Rheometer serial No. ER-406/27. Two pairs of dies were used, each pair having equal radii and different lengths. A diagram of the Davenport Rheometer is shown in Fig. 2.1

2.2.1 Apparatus : The apparatus has four main parts as follows:-

a) a heating chamber.

b) a system to control the temperature of the heating chamber .

c) A motor-driven piston.

d) a pressure measuring system.

The heating chamber contains a heat-conducting barrel, 24-13 cm. long, with a nitride-hardened bore.

The temperature control system was a resistance thermometer forming one arm of an A.C. bridge circuit. The output of the bridge circuit was fed into a phase sensitive amplifier controlling the energy to the heater.

The piston was driven vertically into the barrel by an electronically controlled, variable-speed, D.C. motor.

2.2.2 Method Summary:

The polymer sample was put into the heated barrel containing the extrusion die. The selected extrusion temperature was then precisely controlled and was directly indicated on a mercury-in-glass thermometer residing in the heated chamber. The piston was motor driven vertically into the barrel at a chosen rate. As the polymer was extruded through the die the pressure applied to the sample melt was measured by a transducer inserted in the barrel assembly close to the die and was recorded on an

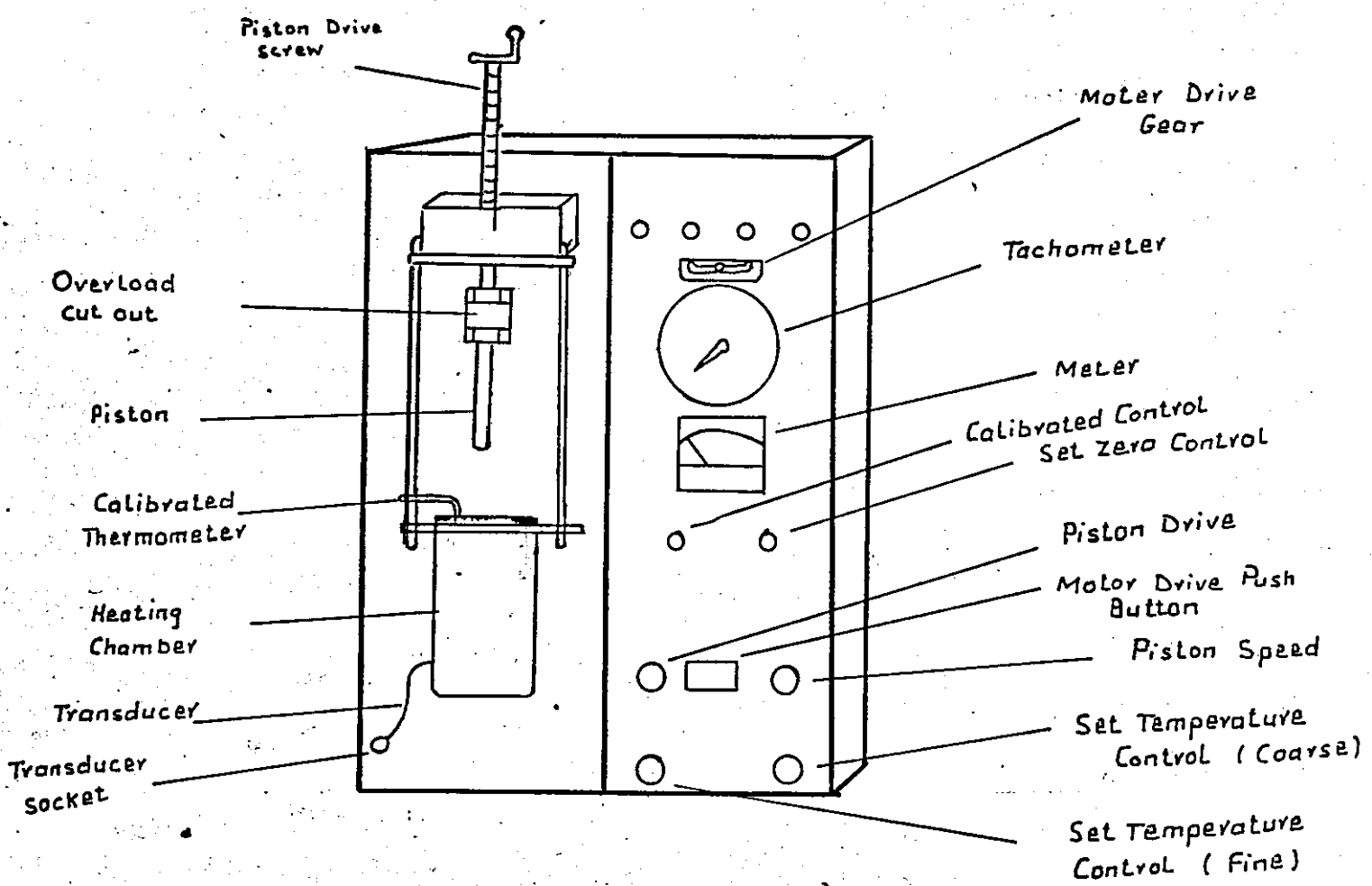

Fig. 2.1:
Davenport Rheometer

electronic strip-chart recorder. The piston speed was then changed to several different rates, the pressure being recorded for each speed. This procedure was repeated at a number of different temperatures (from 150-220^{o}C). The shear-stress and shear-rate were calculated from the piston speed and the corresponding pressures.

Corrections for the entry and exit effects were made by assuming a die of length ($l_1 - l_2$) for which a pressure ($P_1 - P_2$) would be required to give the same output rate (piston speed), where:

l_1, l_2 and P_1, P_2 are, respectively, the lengths (cms) and pressures (p.s.i.) of one pair of die.

On this basis the shear-stress (τ) has been calculated as follows:-

$$\tau = \frac{(P_1 - P_2)r}{2(l_1 - l_2)} \qquad (17)$$

Shear-rate ($\dot{\gamma}$) has been determined from:-

$$\dot{\gamma} = \frac{x}{16.5326.r^3} \qquad (18)$$

where:

r = Capillary radius of each die of one pair of die (cms).

x = Piston drive speed (cm/min)

Table 23 below summarizes the dimensions of the capillary dies used:

Table 23

No.	Die characteristic	r (cms)	l (cms)	l/r
1)	Flat Entry	0.1	2.0	20
2)	Flat Entry	0.1	1.5	15
3)	Flat Entry	0.05	1.5	30
4)	Flat Entry	0.05	1.0	20

2-3 Tubular Film Extrusion

2-3.1 Apparatus :

The line used for film-blow extrusion consisted of a 'Betol' Laboratory Extruder fitted with a conventional polyethylene screen and water cooled feed zone hopper capacity 14 lbs. The die used was a bottom-fed design with 5cms. cord diameter. The length to diameter ratio:

L:D = 20:1

The haul-off section consists of Mobile Film Tower with 12" x 6" diameter rubber covered nip rolls, 5 ft. in height from centre.

Line of the Extruder giving an overall height of 9 ft.

2-3.2 Description of Process :

The equipment shown in the Blown Film Extruder in Fig. (2.2) includes: Extruder, screw, die, cooling ring and wind-up equipment. The extruder may be considered as a hollow cylinder containing a screw, designed with feeding, compression, and metering sections for transport of the polymer. It also had closely controlled heat zones to change the solid polymer to a processable fluid.

The melt emerged from the die in the form of a tube, which was then inflated by air, coming from an air supply, to the desired diameter. The air was entrapped between a set of nip rolls and the extrusion die. As a result the air remained in a constant position and the extruded tube was actually forced over it. The inflated tube was cooled by means of an air cooling ring placed above the die. The tube was then passed between two sets of guiding rolls which flattened it and led it to the nip rolls, where it was pressed completely flat and wound-up in the rolls as a tube.

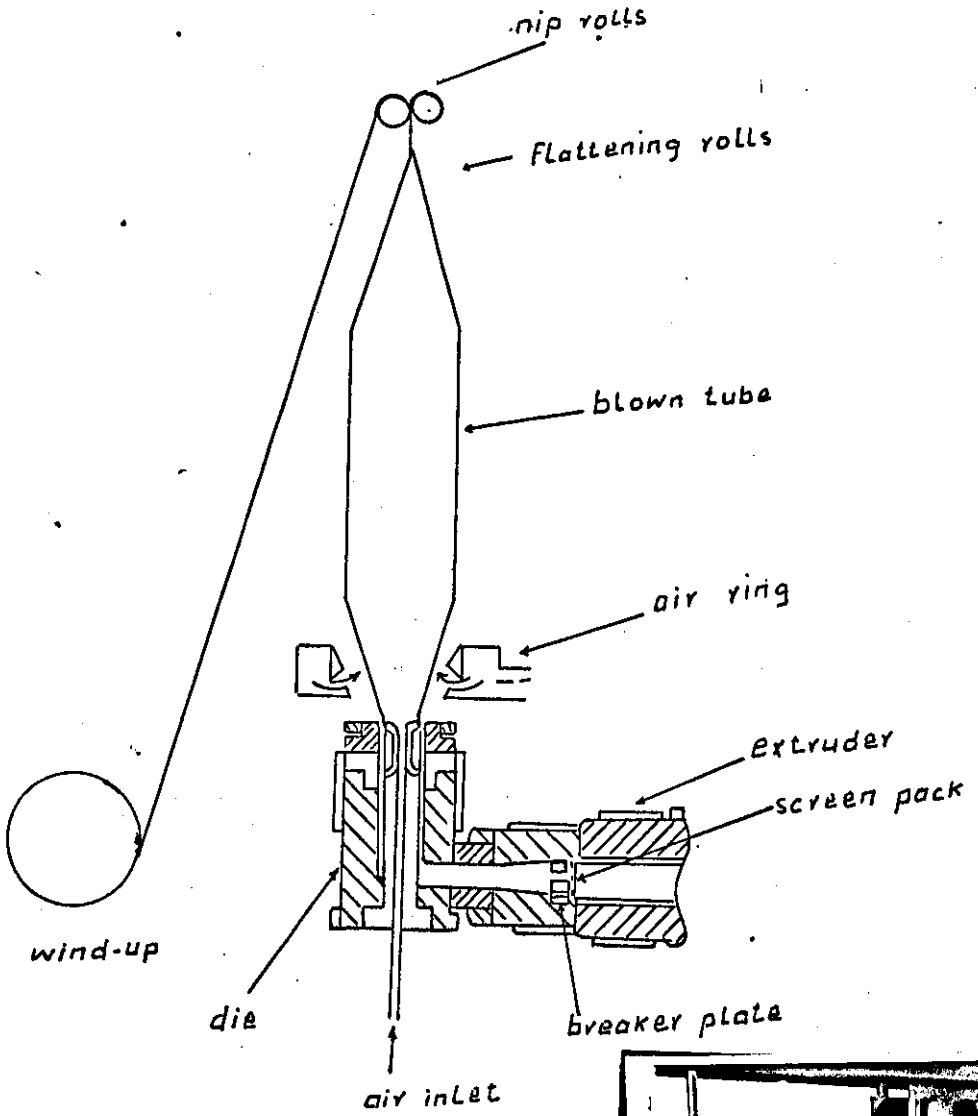

Fig. 2.2. Film-blowing Extrusion.

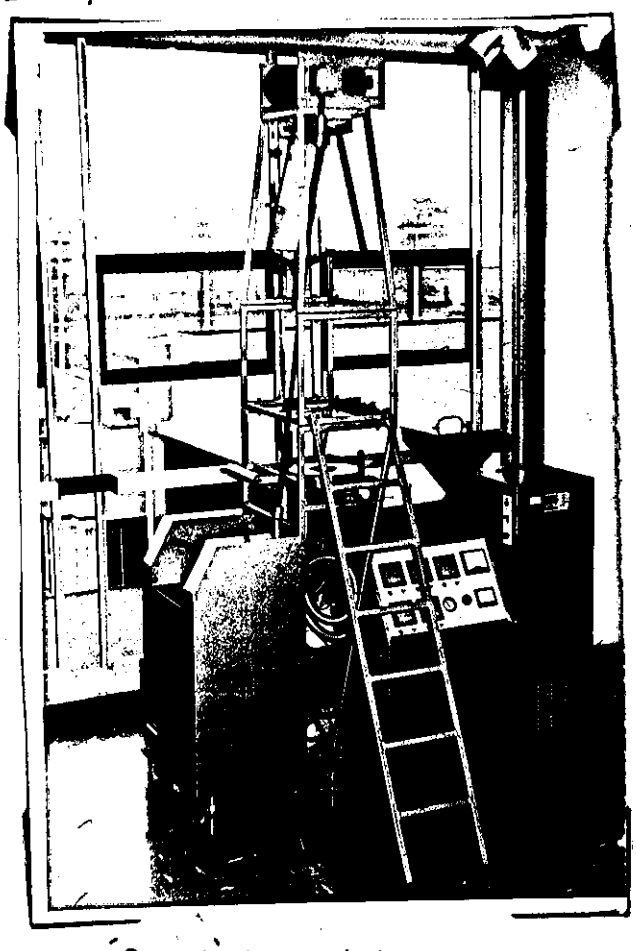

Betol Extruder

2-3.3 Process Variables Investigations :

The process variables investigated were namely:

(i) Haul-off rate.

(ii) Screw speed.

(iii) Blow-up ratio.

The extrusion temperature, freeze-line distance and film thickness were kept constant for the whole sets of experiments. These are summarized in table 2.4 below:-

Table 2.4

Freeze-line distance (cms)	Film thickness (mm)	Extrusion Temperature °C				
		Barrel Zone			Die Zone	
		1	2	3	1	2
25-28	0.060 ± 0.002	155	160	170	190	190

The cooling rate was adjusted when necessary to cope with the increased output rate when the screw speed was increased. The haul-off rate was changed when changing the blow-up ratio or screw speed to give the required film thickness. Each resin was run at the following range of screw speeds and blow-up ratios:-

Screw speeds: 20, 25, 35, 45, 55 (r.p.m)

Blow up Ratios: 0.7, 1.0, 1.4, 1.8, 2.1, 2.4, 2.8

In order to maintain film thickness of 0.006 cms. one set of 35 runs was made for each resin by adjusting the haul-off rate as the blow-up ratio was changed at each constant screw speed. However, it was not possible to work at high blow-up ratios when operating at low screw speeds.

Blow-up ratio was varied by changing film width since dies of different size with identical geometry were not available. By measuring the film width the blow-up ratio was directly determined from the following relation:-

$$\text{Blow-up ratio (B.U.R.)} = \frac{\text{bubble diameter}}{\text{die diameter}}$$

$$= \frac{2 \times \text{blown film width}}{\pi \times \text{die diameter}}$$

2-4 Testing of Film Mechanical Properties

When considering the mechanical strength of film the important factor is the likely durability of film in service, and this factor is almost impossible to access in a simple way. However, it is accepted that a reasonable simulation of the necessary properties can be obtained by measuring the three quantities - tensile strength, impact strength and tear strength. All three properties were measured at room temperature.

2-4.1 Tensile Strength

The tensile strength tests were carried out in Instron Testing Machine (Floor Models TT-B, TT-C1, Standard, Low Speed, Metric) using the ASTM Method, Designation D882, which covers the determination of tensile properties of plastics in the form of thin sheeting (less than 1.0mm. in thickness). Initial strain rate used = 10mm/mm. min.

Method Summary:

A diagram of the Instron Testing Machine is given in Fig. (2.3) The test specimen was placed in the grips of the testing machine, taking care to align the long axis of the specimen with an imaginary line joining the points of attachment of the grips to the machine. The grips were tightened evenly and firmly to the degree necessary to minimize slipping of the specimen during test. The machine was then started and load versus extension was recorded automatically in the chart paper attached.

The tensile strength was calculated by dividing the breaking load (G max.) by the original cross sectional area (Ao) of the specimen:

$$\text{Tensile strength} = \frac{G\ max}{Ao} \qquad \frac{MN}{m^2}$$

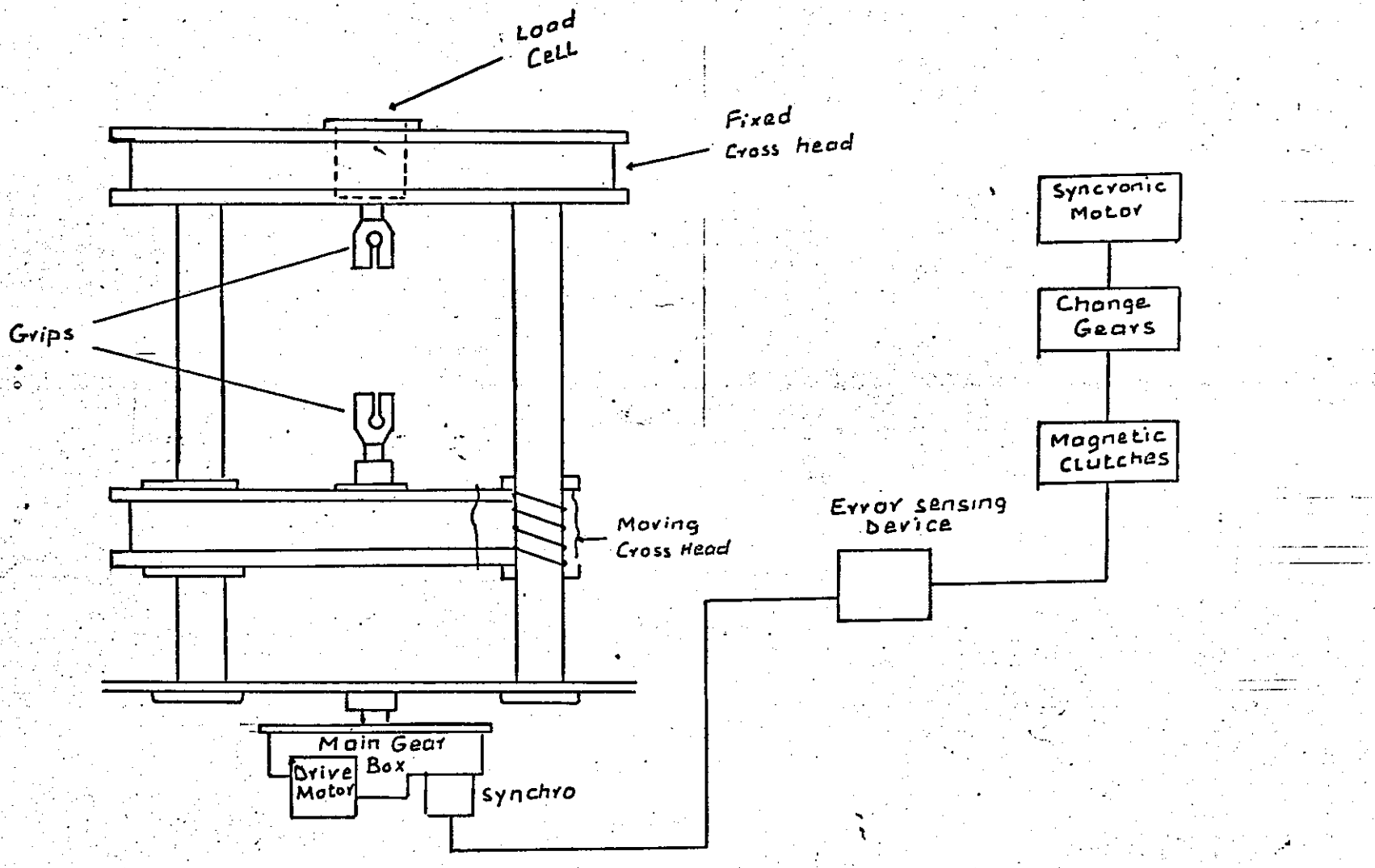

Fig. 23 : Instron Machine (Drive system)

Percentage elongation at break (E) was obtained as follows:

$$E\% = \frac{\Delta l}{l_o} \times 100, \quad \text{where :}$$

Δl = Elongation at the moment of rupture of the specimen.

l_o = initial gauge length of the specimen.

In each test five specimens were used and the arithmatic mean of all values was calculated.

2-4.2 Impact Test:

Impact tests were carried out using the falling dart test, method 306B according to the B.S. 2782. The height of the fall and the mass thereof were altered and the minimum value of the product of fall height and mass which caused fracture was reported as the impact strength of the given material. In each case 20 specimens were used for both trial and testing runs.

Impact Energy = H xW

where:

H = height of fall (cms)

W = the mass (gms)

Impact Strength was calculated as follows:

$$\text{Impact strength} = \frac{1}{20-m} \left\{ \sigma_{m+1} + \sigma_{m+2} \cdots \sigma_{20} \right\}$$

where:

m = number of blows in trial run.

σ_{m+1} = impact energy of first blow of the testing run.

σ_{m+2} = impact energy of 2nd blow of the testing run.

σ_{20} = impact energy of 20th blow of the testing run.

2-4.3 Tear Test

Resistance to tear propagation was determined according to the ASTM method, Designation D1938 which covers the determination of the force in grams necessary to propagate a tear in plastic film (thickness < 1mm) by a single tear method. The tear propagation force was measured using the same Instron Testing Machine which was used for tensile strength test. An initial grip separation of 5cm. and grip separation speed of 25 cm/min. were used to propagate the initiated tear in the specimen. Five specimens were tested in each case and the median of the five maximum tear propagation forces in grams was reported.

2-4.4 Determination of the Birefringence

Birefringence (Δn) was measured using an Eringhaus compensator. Sample strips were prepared from each film grade. The sample investigated was placed on the microscope stage in such a way that the reel edge could be seen. The stage was then rotated and the extinction angle in relation to one direction of the film was recorded. The film was then rotated to 45^{o} position by rotating sample stage. Birefringence was determined by measuring the separation of the two black arcs. By using sodium 'D' line the phase difference was found from compensator settings in calibration tables.

$$\text{Birefringence } (\Delta n) = \frac{\text{phase difference}}{\text{sample thickness}}$$

2.4.5 Determination of FilmDensities :

Film densities were measured in a Density Gradient Column using ethyl alcohol and boiled distilled water, and standard floats having densities in the range:

0.9150 - 0.9500

The positions of the floats were determined with the aid of a cathetometer, measuring at the centre of volume. Those were marked on a graph and the best straight line was drawn. Samples were then cut from each film and then inserted in the column. After allowing the specimens to reach equilibrium, their positions were measured and the corresponding densities were then obtained from the graph.

2.4.6 Determination of the Critical shear-rate

The critical shear-rate ($\dot{\gamma}_c$) was determined for each temperature as the maximum shear-rate after which fracture of the extrudate of the given polymer grade occurred. All measurements of the critical shear-rate were made using die No. (1) in table (2.3).

Experimental Error

It is essential to have estimate of the experimental error associated with the various procedures and testing methods. These can be grouped as follows:

a) Errors arising from shear-stress shear-rate measurements.

b) Errors arising from measurements of strength properties of the end films, and these are mainly tensile and tear strength properties. As impact strength is estimated from a set of test trials, the main error can arise from slippage of the test specimen at the moment of impact. To minimize this a rough rubber ring was placed between the specimen and the support.

Experimental error in both cases is assessed by a measurement of the estimated standard deviation (S) from the following relationship:-

$$S = \sqrt{\frac{\Sigma x^2 - n\bar{x}^2}{n-1}}$$

where:-

x = value of a single observation

$\bar{x}$ = arithmatic mean of the set of observations

n = number of observations

The following table summarises the range of experimental errors as estimated by the standard deviation (S) from the sets of observations carried out to characterize:

a) Flow properties of the polyethylene grades.

b) Tensile and tear strength properties of the different films produced.

Errors of the equipment used are also incorporated in this table:-

Table: 2.5

	Source of Error	Degree of Error	Property investigated	Number of trials	Range of S					
					XJF/46/41	XJF/46/63	MS/5	MS/25	MS/50	MS/100
(a)	(0-3000) psi Transducer	± 3%	Shear-stress shear-rate dependence	3 (each trial with 4 dies).	1.0-1.8	1.1-1.7	1.1-1.9	1.3-1.8	0.9-1.5	1.0-1.7
	Mercury-in-glass Thermometer	± 5°C								
(b)	Instron Testing Instrument	Accuracy of overall load-weighing system is ± ½% of indicated load.	Tensile Strength	5 for each case	2-4.5	2.4-4.2	3.1-4.6	2.3-3.8	2.9-4.1	2.8-4.9
			Tear Propagation	5 for each case	16 - 27.5	15.5 - 24.5	14.5 - 26.5	15.5 - 28	14.5 - 25	16 - 26

Section 3

Results:

Introduction:

In this section the results obtained from the flow properties measurements and the tests carried out for determination of mechanical properties of the different films are given. The detailed consideration of the interaction of the various results is deferred to the Discussion - Section 4.

The data obtained describing the relationship of the tensile, tear and impact strengths of films made from the high and the low slip grades (MS/100 and MS/5) with blow-up ratio and screw speed were computed in an I.C.L. Computer using the method of least squares.

This section can be divided into two main parts:

a) Flow properties investigations.

b) Effect of extrusion conditions on the mechanical properties of the end films.

3-1 Flow Properties Investigations :

The flow data obtained using the pressure substraction method, described previously in section 2, to correct for entry and exit effects have shown excellent superimposition for the two pairs of dies used. This can be taken as a good evidence to assume absence of slip at the wall of the tube throughout the whole set of experiments carried out.

3-1-1 Shear-Stress Shear-Rate Dependence

Shear-stress shear-rate data are illustrated in table 3.1. Fig. 3.1 shows the family of flow curves obtained at different temperatures, respectively, for the two standard polyethylene grades (Fig. 3.1,a) and

the four grades prepared by the incorporation of additives (Fig. 3.1, b, c, d, e, f).

For all grades, at 150°C, plots of log shear-stress (τ) versus log shear-rate ($\dot{\gamma}$) are linear over the entire range measured. This linearity, however, tends to decrease with increasing temperature and shear-rate.

In order to explain the mutual positioning of the curves at various shear-rate and temperature ranges, it was necessary to consider the shear-rate dependence of the apparent power law exponent (n), which is illustrated in table 3.2. From this it can be seen that n is only constant over a narrow range of $\dot{\gamma}$. The degree of non-Newtonian flow behaviour is seen to decrease with decreasing $\dot{\gamma}$ and with increasing temperature.

It is apparent from table (3.2) and fig. (3.1 (e.f.)) that at the high temperature range (205, 220)°C , melt flow of the low density polyethylene samples differ significantly in the degree of non-Newtonian behaviour, depending on the quantity of the slip agent added. The lower the slip the stronger is the shear-rate dependence of the apparent power law exponent (n). However, at 205°C and 220°C and $\dot{\gamma}$ range of (500-1000) sec^{-1}, the high slip grades are less non-Newtonian than the low slip ones.

Table 3.1 : Flow properties data of L-D-Polyethylene grades:
(a,b) Standard polyethylene grades
(c,d,e,f) Prepared samples

(a)

t^{o}_{c}	$\dot{\gamma}$ sec^{-1}	τ , p.s.i.	$\mu \times 10^{3}$ poise	$\dot{\gamma}_c$, sec^{-1}
		XJF/46/41		
	16.6	9.8	42.0	
	23.2	10.9	32.3	
150	33.3	12.0	25.0	
	49.9	13.4	18.5	
	66.5	15.6	16.2	
	82.2	17.6	14.6	96.5
	16.6	7.5	31.2	
	33.3	10.0	20.7	
	49.9	12.1	16.7	
175	66.5	13.2	13.7	233.1
	99.8	15.0	10.4	
	116.4	15.6	9.4	
	166.3	17.9	7.4	
	16.6	4.2	17.5	
	49.9	7.2	9.9	
	66.5	9.4	9.0	
190	83.2	9.7	8.0	
	99.8	10.9	7.5	400
	133.1	13.1	6.8	
	249.5	16.9	4.9	
	266.1	17.6	4.6	
	33.3	3.8	7.9	
	49.9	5.3	7.3	
	83.2	6.4	5.3	
	166.3	9.4	3.9	582
205	332.7	13.6	2.8	
	532.3	15.0	1.9	
	16.6	2.9	12.0	
	49.9	5.0	6.9	
	99.8	8.1	5.6	998
220	166.3	10.9	4.5	
	332.7	14.0	2.9	
	499	16.0	2.2	
	665.4	17.9	1.9	
	930	19.8	1.5	

Table 3.1 : (b)

$t^{o}c$	$\dot{\gamma}$, sec^{-1}	τ , p.s.i.	$\mu \times 10^{3}$ poise	$\dot{\gamma}c$, sec^{-1}
		XJF/46/63		
	16.6	8.8	36.6	
	33.3	11.6	24	
150	49.9	13.4	18.5	166.3
	66.5	15.1	15.7	
	99.8	17.8	12.3	
	116.4	18.5	11.0	
	133.1	19.5	9.0	
	16.6	6.7	27.8	
	49.9	11.6	16.0	
175	83.2	13.0	10.8	
	99.8	14.6	10.1	299.4
	133.1	15.6	8.1	
	249.5	19.6	5.4	
	16.6	5.8	24.0	
	33.3	6.8	14.1	
	66.5	10.0	10.4	
190	99.8	11.6	8.0	
	133.1	13.6	7.1	581.9
	249.5	15.1	4.2	
	332.7	18.0	3.7	
	400.0	19.5	3.4	
	520.0	22.0	2.7	
	16.6	4.7	19.6	
	33.3	5.3	10.5	
	66.5	7.2	7.5	
205	133.1	10.3	5.3	
	249.5	12.8	3.5	831.7
	332.7	14.4	3.0	
	499	16.8	2.3	
	798.4	19.0	1.6	
	16.6	2.7	10.9	
	33.3	3.9	8.0	
	66.5	6	6.2	
	99.8	8.6	5.9	1164.4
	133.1	10.0	5.7	
220	166.3	10.3	4.3	
	249.5	12.9	3.6	
	499	17	2.4	
	665.4	18.8	2.0	
	930.1	20.9	1.6	

Table: 3.1 : (c)

Temp. °c	$\dot{\gamma}$, sec^{-1}	τ, p.s.i.	$\mu \times 10^{-3}$ poise	$\dot{\gamma}_c$, sec^{-1}
		XJF/5		
150	16.6	7.2	29.9	
	23.3	8.6	25.5	
	33.3	9.8	20.3	73.8
	49.9	11.9	16.5	
	66.5	13.7	14.2	
	73.7	15	12.4	
175	16.6	5.3	22.0	
	33.3	7.8	16.2	
	49.9	9.2	12.7	
	66.5	10.5	10.9	199.6
	99.8	12.8	8.8	
	133.1	14.5	7.5	
	166.3	16.1	6.7	
190	16.6	3.7	15.4	
	33.3	5.6	11.6	
	49.9	7	9 .7	413
	99.8	9.4	6.5	
	133.1	12	6.2	
	166.3	12.7	5.7	
	332.7	17.2	5.3	
	499.5	21.1	2.9	
205	16.6	3.1	10.7	
	23.2	3.6	12.9	
	33.3	4.1	8.5	665
	66.5	6	6.2	
	133.1	8.8	4.6	
	249.5	11.5	3.2	
	499	13.4	1.9	
	665	14.1	1.5	
220	16.6	2.3	9.6	
	23.2	3.1	9.2	
	49.9	5.0	6.9	915
	99.8	6.8	4.7	
	166.3	9.7	4.0	
	332.7	12.9	2.7	
	499	14.2	2.0	
	665.4	15.4	1.6	
	798.4	15.7	1.4	

Table: 3.1 : (d)

Temp. °C	$\dot{\gamma}$, sec^{-1}	τ, p.s.i.	μ x 10^3 poise	$\dot{\gamma}_c$, sec^{-1}
		XJF/25		
150	16.6	6.8	28.3	83.2
	23.3	8.3	24.6	
	33.3	9.3	19.9	
	49.9	11.1	15.3	
	66.5	13.0	13.5	
	83.2	14.3	11.9	
175	16.6	5.3	22.0	233
	33.3	7.2	14.9	
	49.9	8.6	11.9	
	83.2	11.5	9.5	
	99.8	12.2	8.5	
	133.1	13.9	7.2	
	166.3	15.2	6.3	
190	16.6	3.5	14.6	499
	33.3	5.0	10.4	
	49.9	6.3	8.7	
	83.2	8.8	7.3	
	133.1	11.6	6.0	
	249.5	15.0	4.2	
	332.7	16.6	3.4	
	499	20.1	2.8	
205	16.6	2.9	12.1	732
	33.3	4.5	9.3	
	49.9	5.4	7.5	
	99.8	7.5	5.2	
	166.3	9.2	3.8	
	332.7	12.4	2.6	
	499	14.0	1.9	
	665.4	15.1	1.6	
220	16.6	2.4	10.0	998
	33.3	3.8	7.9	
	49.9	4.6	6.4	
	99.8	7.0	4.8	
	133.1	8.4	4.4	
	166.3	9.4	3.9	
	249.5	11.3	3.2	
	332.7	12.4	2.6	
	665.4	14.8	1.5	
	798.4	15.0	1.3	

Table 3.1 : (e)

Temp. °C	$\dot{\gamma}$, sec^{-1}	τ, p.s.i.	μ x 10^{3} poise	$\dot{\gamma}_c$, sec^{-1}
		XJF/60		
150	16.6	6.3	26.2	99.8
	23.2	7.6	22.7	
	33.3	9	18.6	
	49.9	10.5	14.5	
	66.5	12.8	13.3	
	83.2	14.0	11.6	
	99.8	15.0	10.4	
175	16.6	4.9	20.5	300
	33.3	6.8	14.1	
	66.5	10.0	10.4	
	83.2	10.8	9.0	
	99.8	11.5	7.9	
	133.1	13.1	6.8	
	166.3	14.0	5.8	
	249.5	17.0	4.7	
190	16.6	3.3	13.7	583
	33.3	5.4	11.2	
	66.5	6.9	7.2	
	99.8	9.0	6.2	
	133.1	11.0	5.7	
	166.3	12.1	5.0	
	332.7	15.9	3.3	
	499	18.5	2.6	
205	16.6	2.8	11.6	831
	33.3	4.3	8.9	
	66.5	5.6	5.8	
	99.8	7.8	5.4	
	166.3	9.9	4.1	
	332.7	13.1	2.7	
	499	15.0	2.1	
	798.4	17.7	1.5	
220	16.6	2.2	9.1	1160
	33.3	3.5	7.3	
	66.5	5.3	5.5	
	99.8	6.3	4.4	
	133.1	7.8	4.0	
	166.3	8.4	3.5	
	332.7	11.7	2.4	
	499	13.5	1.9	
	930.1	16.0	1.2	

Table: 3.1 : (f)

Temp. °C	$\dot{\gamma}$, sec^{-1}	τ, p.s.i.	μ x 10^3 poise	$\dot{\gamma}_c$, sec^{-1}
		XJF/100		
150	16.6	5.3	22.0	116.4
	33.3	7.8	16.2	
	49.9	9.0	12.4	
	66.5	10.2	10.6	
	83.2	11.3	9.4	
	99.8	12.7	8.8	
	116.4	13.3	7.9	
175	16.6	4.4	18.3	333
	33.3	5.6	11.6	
	49.9	7.5	10.4	
	83.2	9.9	8.2	
	99.8	10.6	5.5	
	133.1	12.7	6.6	
	166.3	13.5	5.6	
	249.5	16.0	4.5	
190	16.6	3.1	12.9	600
	33.3	4.5	9.3	
	49.9	5.6	7.7	
	66.5	6.4	6.6	
	99.8	8.4	5.8	
	166.3	10.5	4.4	
	332.7	15.0	3.1	
	499	17.6	2.4	
205	16.6	2.6	10.8	915
	33.3	3.8	7.9	
	66.5	5.0	5.2	
	99.8	6.2	4.3	
	133.1	7.4	3.8	
	199.6	9.5	3.3	
	332.7	11.0	2.3	
	499	12.8	1.8	
	665.4	13.8	1.4	
	798.4	15.0	1.3	
220	16.6	2.0	8.3	1331
	33.3	2.9	6.0	
	66.5	5.0	5.2	
	133.1	7.3	3.8	
	166.3	8.0	3.3	
	199.6	8.6	3.0	
	332.7	10.9	2.3	
	499	13.0	1.8	
	665.4	13.9	1.4	
	930.1	15.3	1.2	

Table 3.2 :

Variation of apparent power law exponent, n, with shear rate, $\dot{\gamma}$, and temperature, (t)

$t^{o}c$	Range of $\dot{\gamma}$, sec^{-1}	Power Law exponent, (n)					
		XJF/5	XJF/25	XJF/50	XJF/100	XJF/46/41	XJF/46/63
150	10 - 50	0.48	0.49	0.48	0.49	0.44	0.51
	50 - 100	0.48	0.48	0.52	0.48	0.44	0.44
175	10- 50	0.52	0.52	0.56	0.56	0.48	0.52
	50 - 100	0.48	0.48	0.52	0.52	0.37	0.37
	100 - 500	0.41	0.40	0.41	0.46	0.33	0.32
190	10 - 50	0.51	0.53	0.59	0.58	0.60	0.57
	50 - 100	0.52	0.50	0.54	0.57	0.63	0.52
	100 - 500	0.44	0.43	0.44	0.47	0.41	0.40
	500 -1000	0.37	0.33	0.26	0.22		
205	10 - 50	0.59	0.56	0.57	0.57	-	-
	50 - 100	0.52	0.52	0.56	0.55	0.65	0.56
	100 - 500	0.36	0.38	0.46	0.46	0.48	0.40
	500 -1000	0.16	0.19	0.33	0.36	0.39	0.37
220	10 - 50	0.67	0.67	0.65	0.62	-	-
	50 - 100	0.59	0.56	0.55	0.59	0.66	0.63
	100 - 500	0.43	0.44	0.45	0.45	0.46	0.41
	500 -1000	0.15	0.16	0.32	0.38	0.36	0.37

Fig. 3.1 'a'

Shear-stress(τ) shear-rate($\dot{\gamma}$) dependence

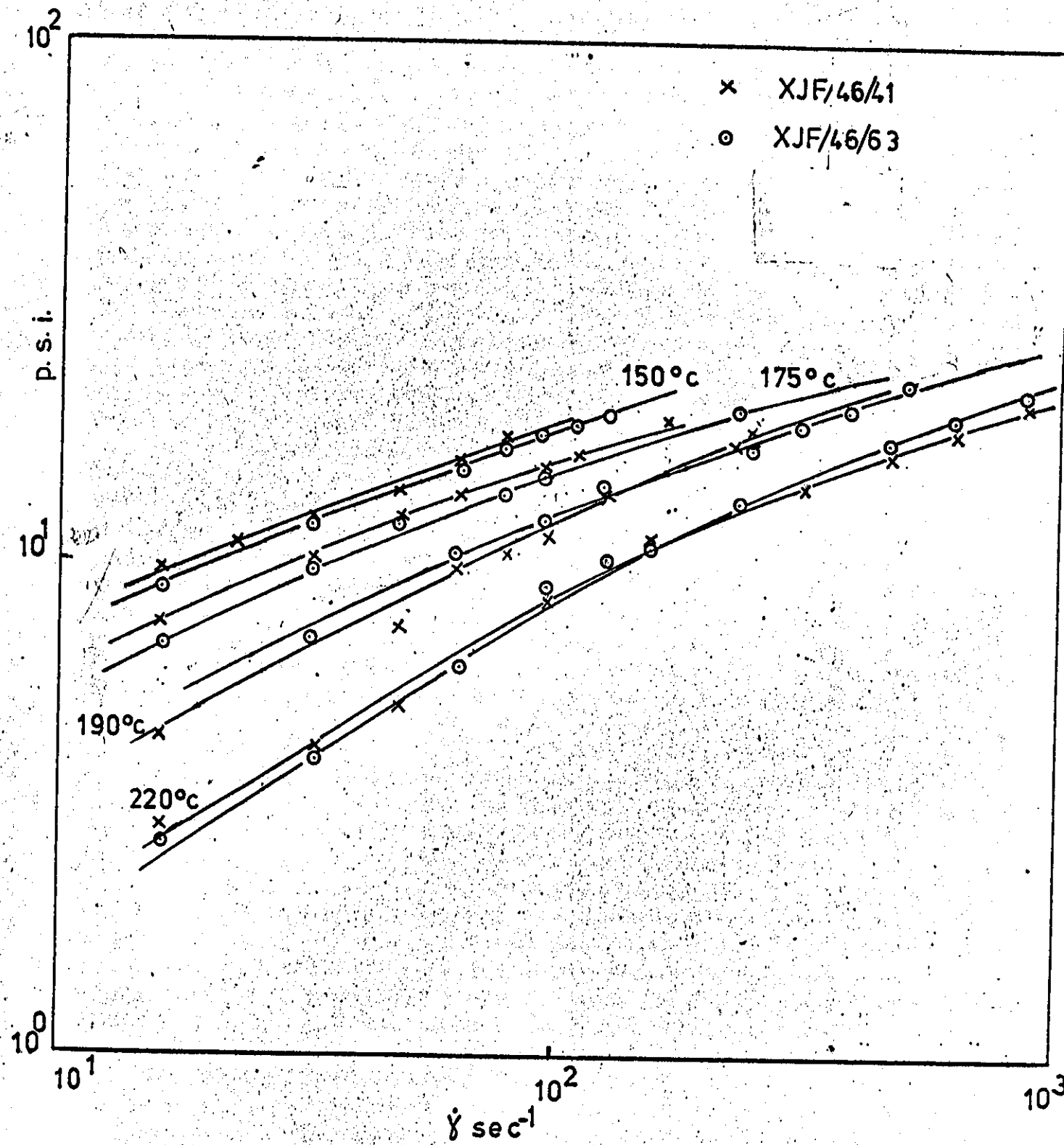

Fig. 3.1 'b':

Shear-stress(τ) shear-rate($\dot{\gamma}$) dependence

$t = 150^{\circ}c$

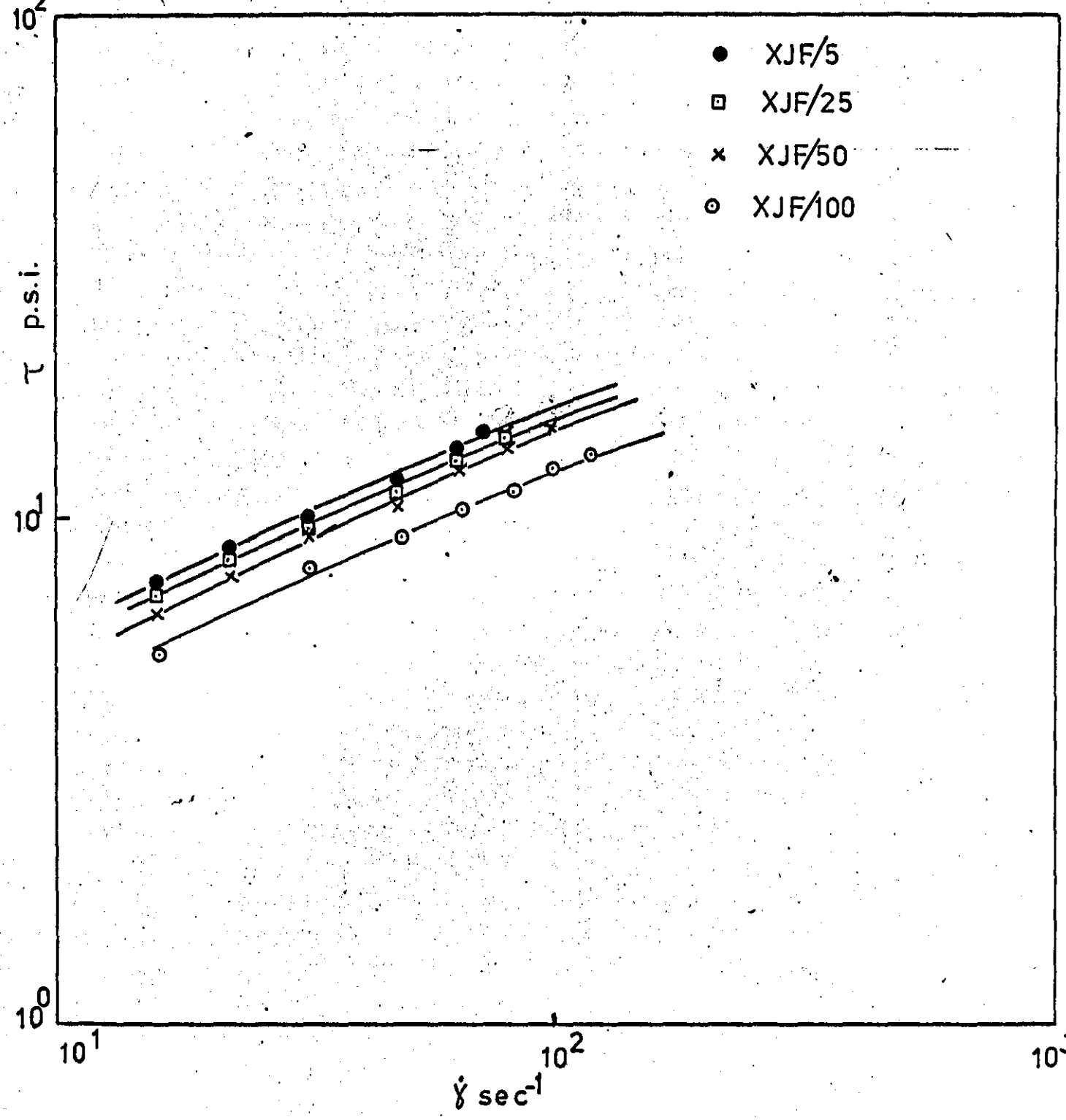

Fig. 3.1 'c' :

Shear-stress(τ) shear-rate($\dot{\gamma}$) dependence

$t = 175°c$

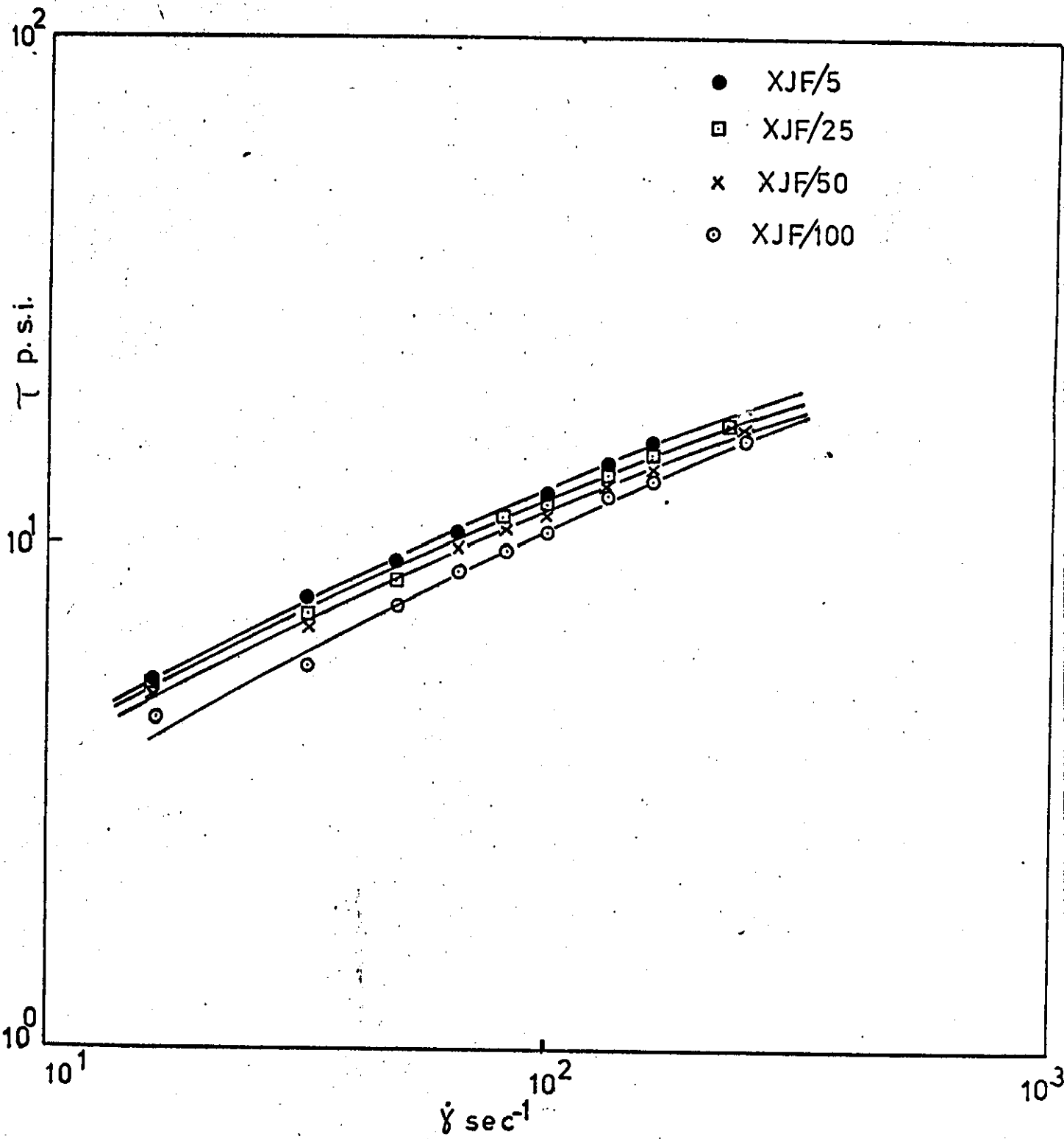

Fig. 3.1 'd':

Shear-stress(τ) shear-rate($\dot{\gamma}$) dependence

t = 190°c

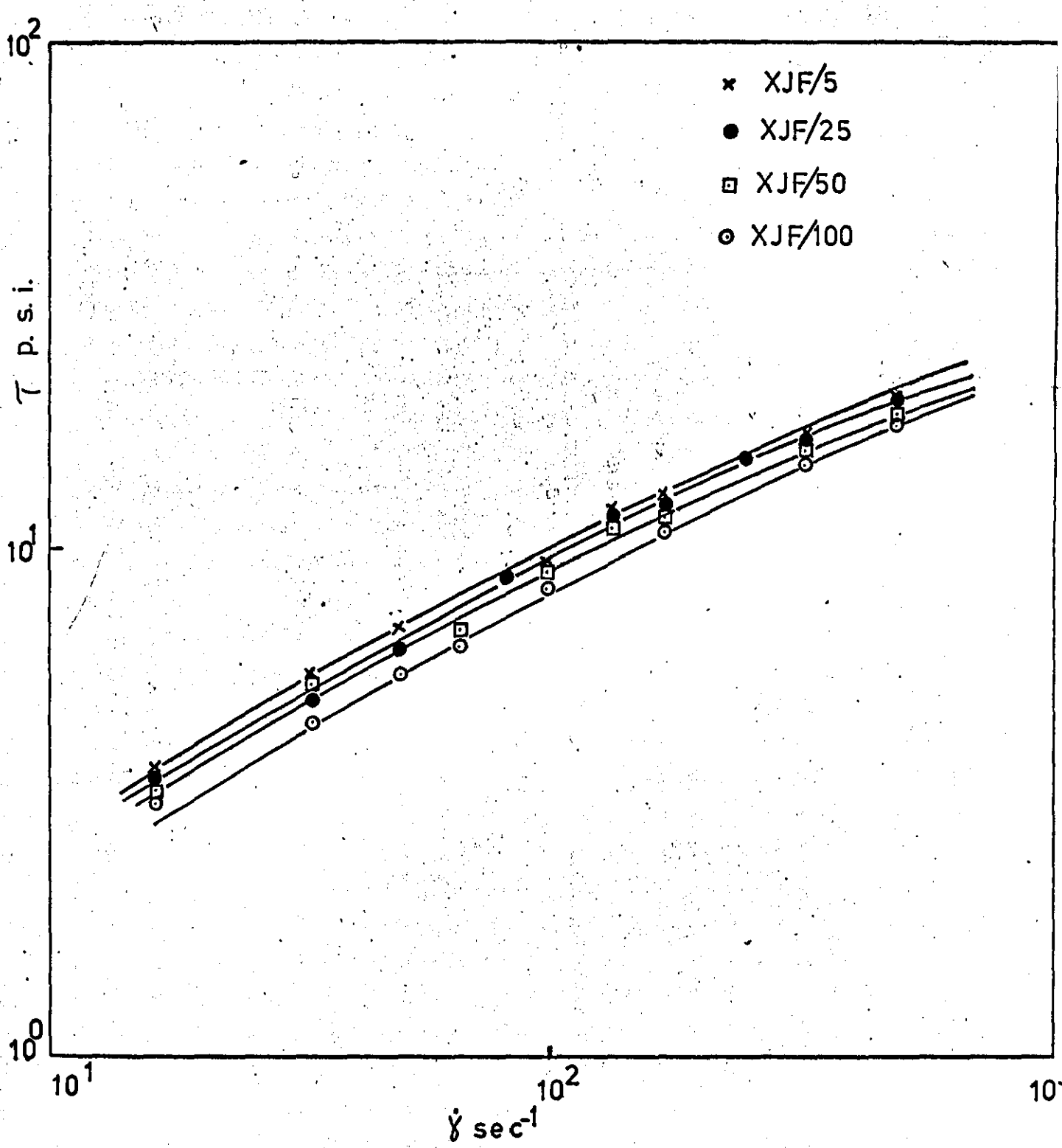

Fig. 3.1 'e'

Shear-stress(τ) shear-rate($\dot{\gamma}$) dependence

t = 205°c

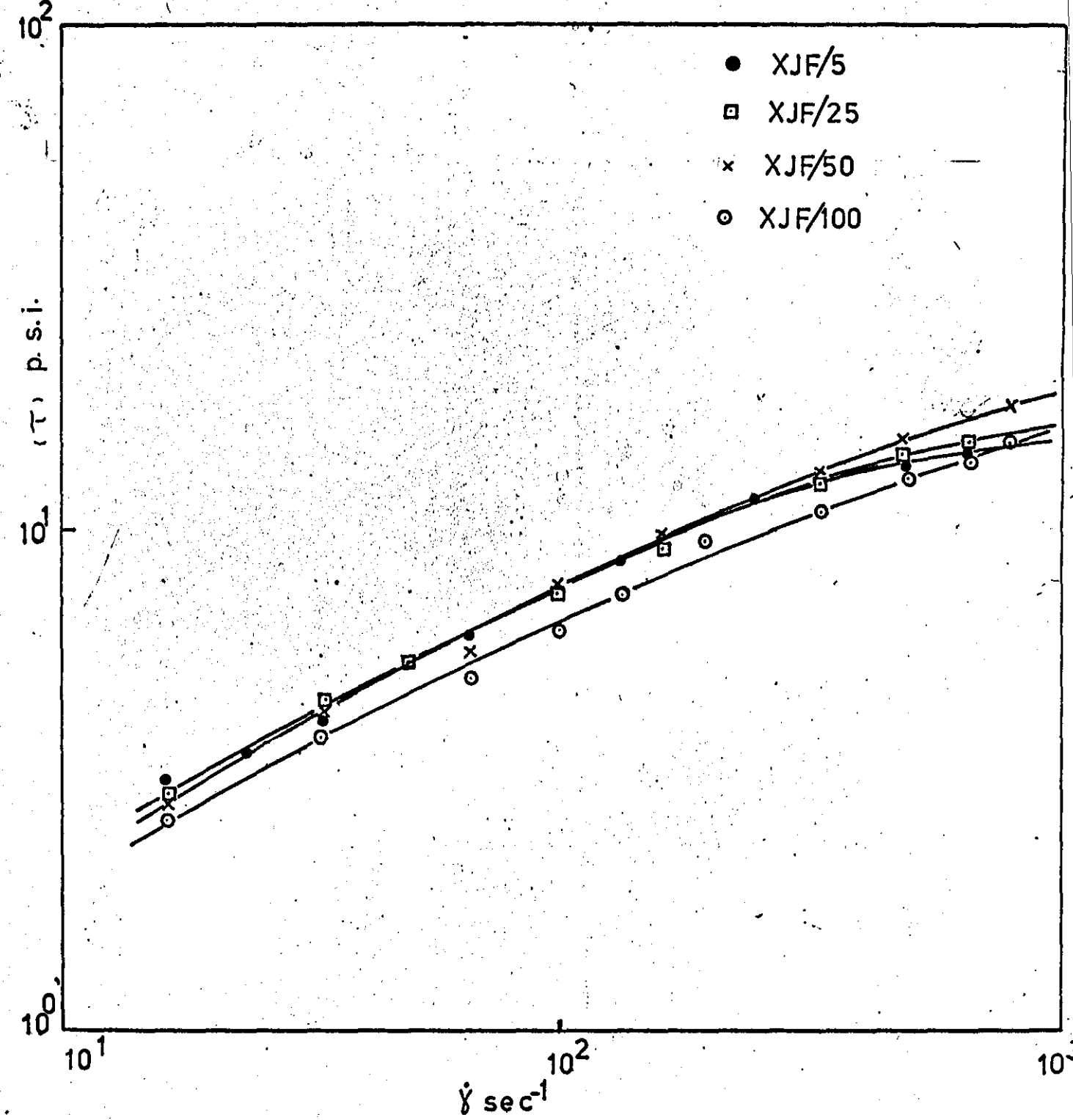

Fig. 3.1 : 'f'

Shear-stress(τ) shear-rate($\dot{\gamma}$) dependence

$t = 220^{\circ}c$

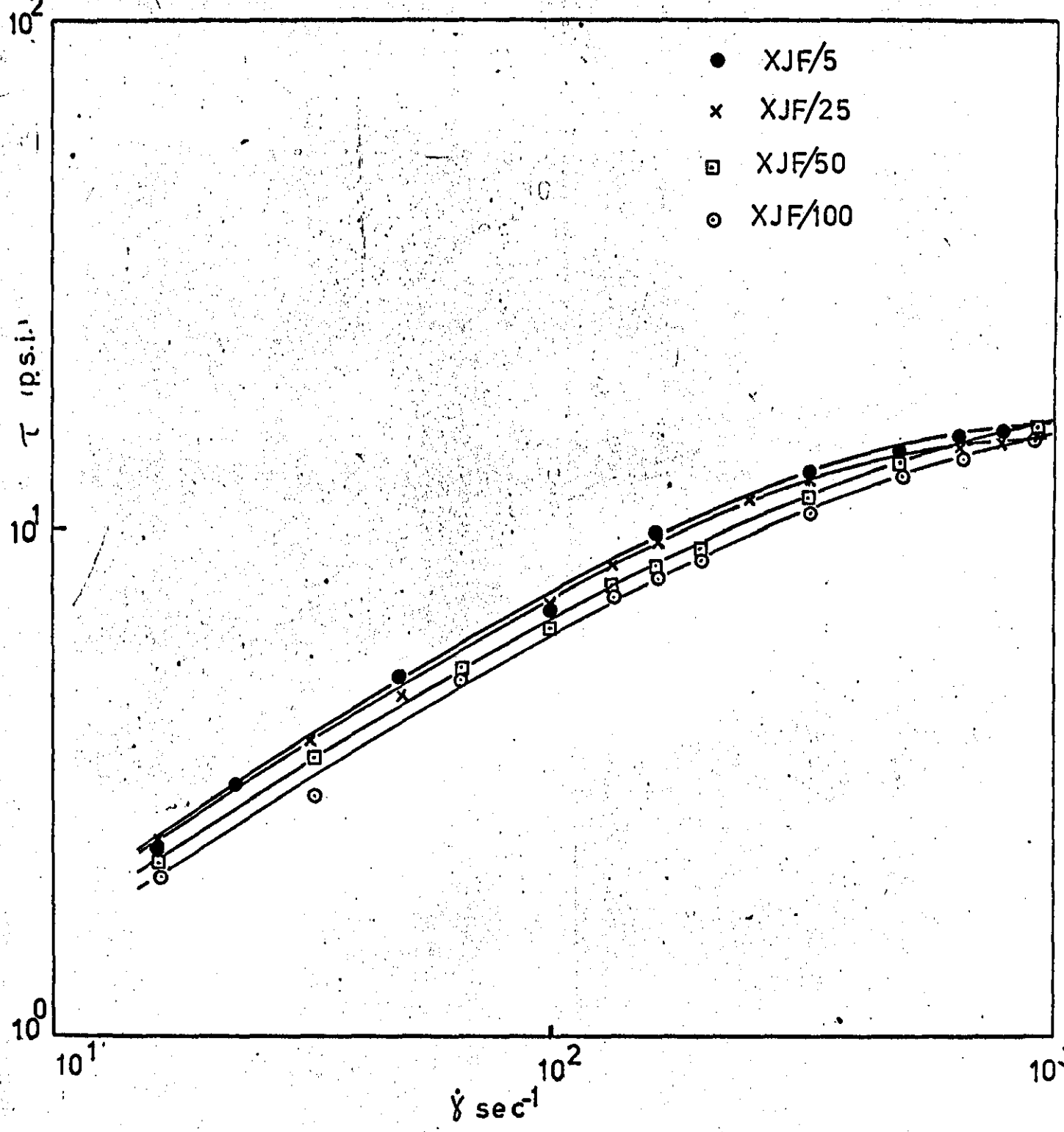

3-1.2 Shear-rate Dependence of Melt Viscosities

The apparent melt viscosity (μ) was quoted as the relationship of the shear-stress (τ) to the shear-rate ($\dot{\gamma}$), i.e.

$$\mu = \frac{\tau}{\dot{\gamma}} \quad \ldots$$

The shear-rate dependence of the apparent melt viscosities is shown in table (3.1), and data from this table were plotted in fig. (3.2, a,b).

The data confirm the well-known fact that apparent melt viscosity decreases with increasing temperature and shear-rate.

As can be seen from fig. 3.2 from a comparison of the apparent melt viscosities of the polyethylenes at different temperatures, the low slip grade (MS/5) displayed the highest melt viscosity at 150°C, followed by the other grades, respectively in increasing order of slip, i.e. the lowest melt viscosity was displayed by the highest slip grade (MS/100).

However, with increasing temperature and shear-rate this difference in the apparent viscosities becomes less significant and at temperature 220°C and shear-rate 1000 sec^{-1}, they all almost exhibit equal melt viscosities.

Fig. 3.2 a.

Variation of viscosity (μ) with shear rate ($\dot{\gamma}$) and temperature

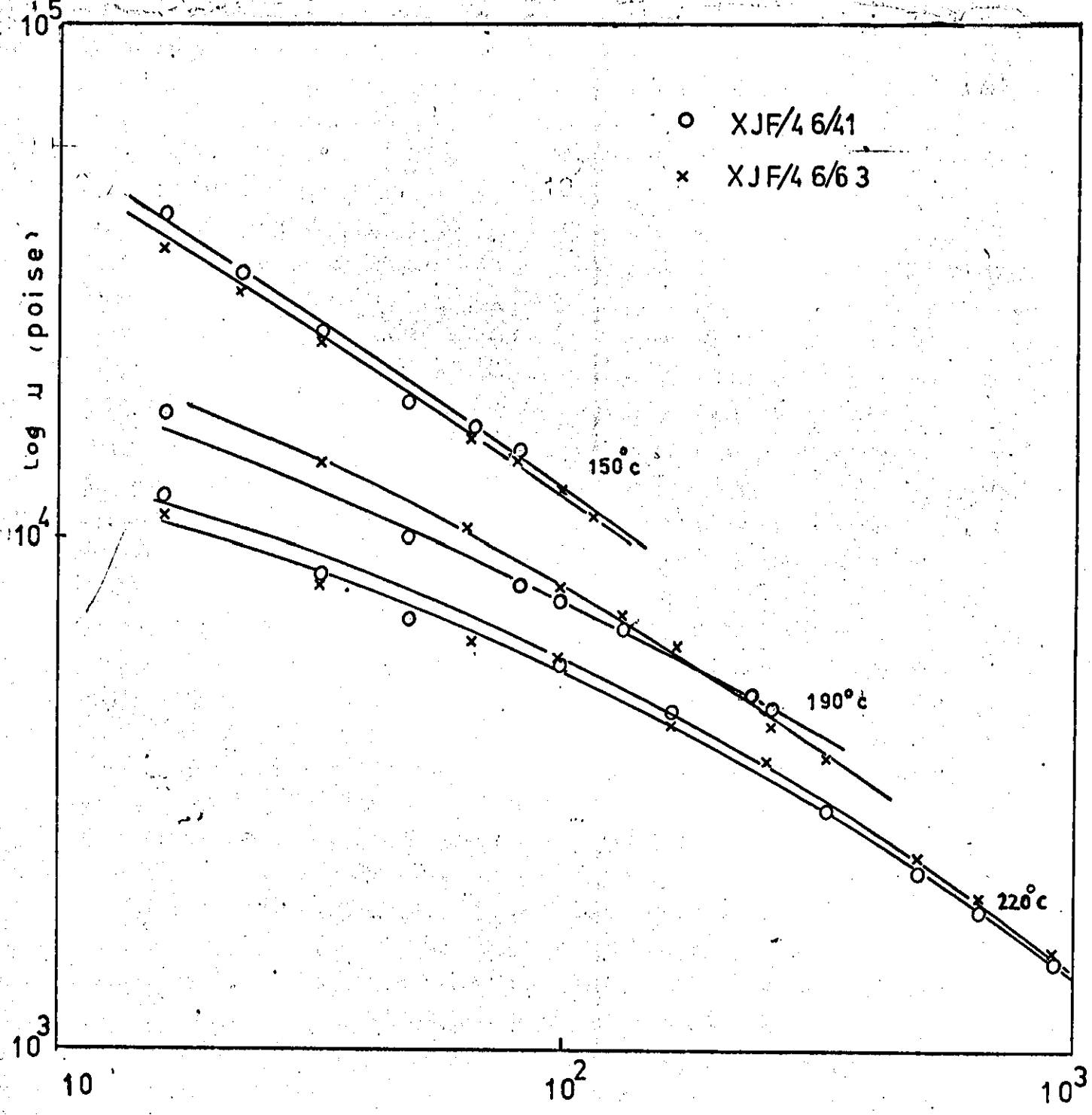

Fig.3.2'b'.

Variation of viscosity(u) with shear rate($\dot{\gamma}$) and temperature

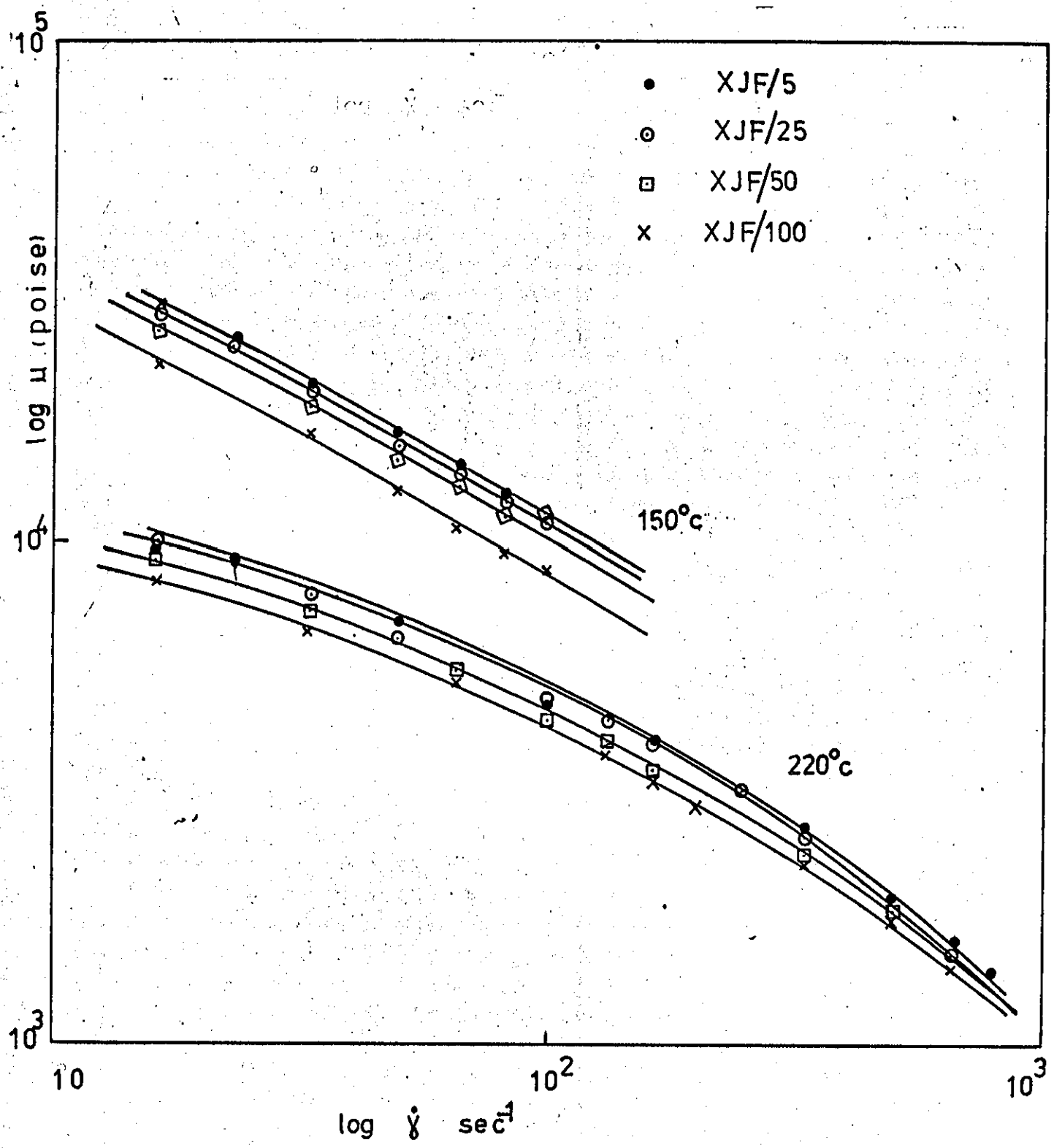

3-1.3 Critical Shear-rate :

The temperature dependence of the critical shear-rate ($\dot{\gamma}_c$) of the polyethylene grades is shown in table (3.1). Data from this table were plotted in fig. 3.3. It can be seen that, for all grades, increasing the temperature gave a higher critical extrusion rate before turbulence or fracture of the extrudate. The critical shear-rate ($\dot{\gamma}_c$) increased gradually with temperature up to near 190°C after which it started to rise sharply.

Effect of the degree of slip on the critical shear-rate can also be seen from fig. 3.3. The high slip grade (MS/100) displayed the highest critical shear-rate for the whole range of temperatures investigated, followed by the medium slip grade (MS/50), then the medium-low slip (MS/25) and finally the low slip (MS/5), which displayed the lowest critical shear-rate value.

Fig.3.3: Variation of critical shear-rate ($\dot{\gamma}_c$) with temperature (t).

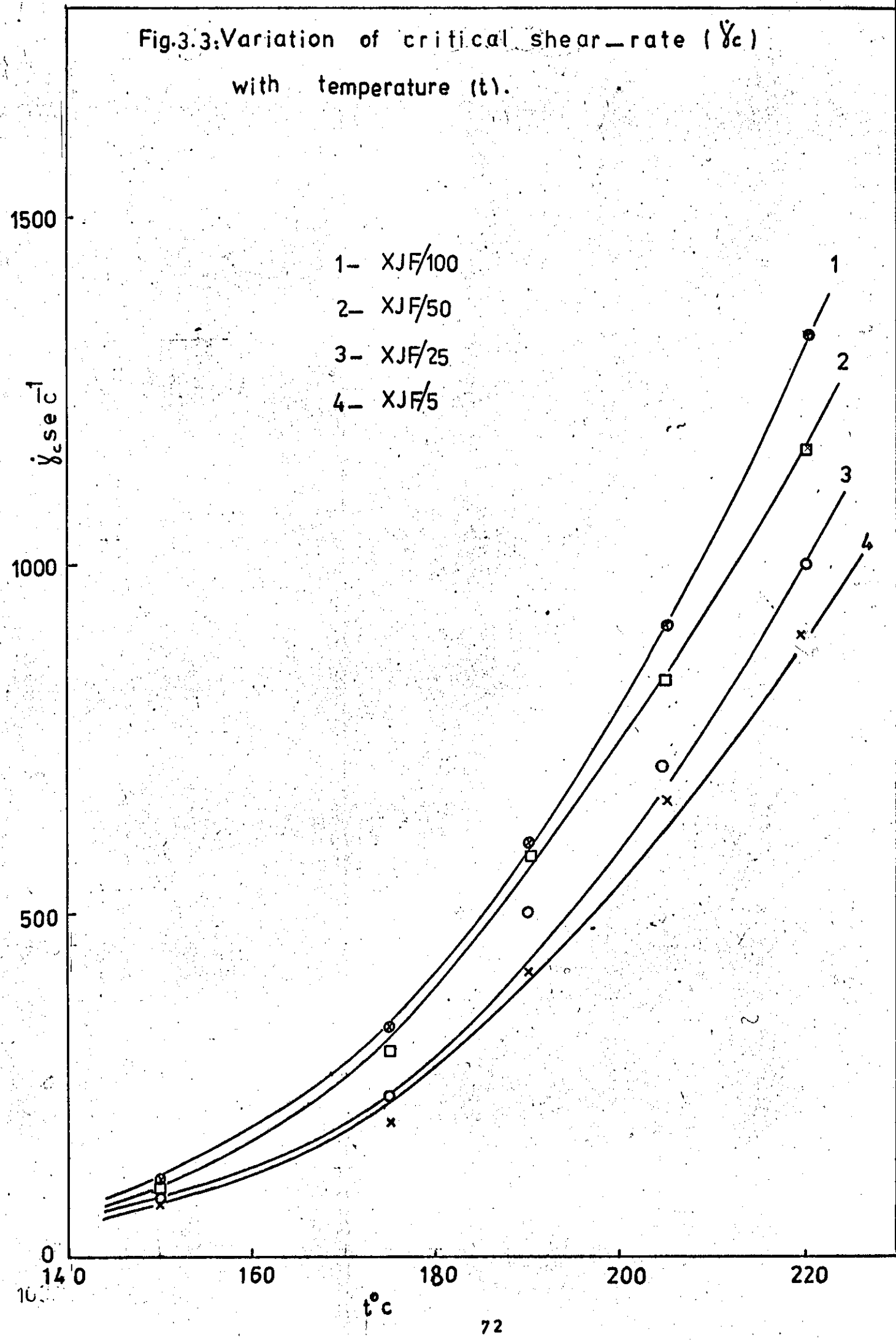

3-1.4 Apparent Energy of Activation :

Temperature-dependence of the apparent melt viscosity is related to the apparent energy of activation for viscous flow (ΔE), defined by the Arrhenius equation (equation 11). Since A is treated as a constant, ΔE for non-Newtonian systems is a function of shear-rate or shear-stress. According to the method of Bestul and Belcher apparent activation energies for viscous flow were calculated at fixed rates of shear and at fixed shear-stresses as follows:

The shear-stress (τ) versus shear-rate ($\dot{\gamma}$) was plotted at the temperatures investigated (150, 175, 190, 205, 220)^{o}C. A line representing a constant shear-rate $\dot{\gamma} = 50\ sec^{-1}$ was drawn and the slopes of the tangents at the points of intersection were determined. These slopes gave the viscosities at constant shear-rate.

Using equation (11), the logarithm of the apparent viscosity (μ) at constant shear-rate was plotted against the reciprocal of temperature (1/T).

The same procedure was repeated at the following shear-rates:

$\dot{\gamma} = (200,\ 500,\ 800) sec^{-1}$

Similarly, by drawing a line representing a constant shear-stress $\tau = 5.6$ p.s.i., and following the same procedure as above, the logarithm of the apparent melt viscosity at constant shear-stresses ($\tau = 5.6, 9, 12, 16$) p.s.i.) was plotted against (^{1}/T).

These plots, which are shown in fig. 3.4 (a,b,c,d,e,f,) are approximated by straight lines from the slope of which ΔE was calculated.

Apparent activation energies at constant shear-stress (ΔE_{τ}) and constant shear-rate ($\Delta E_{\dot{\gamma}}$) are illustrated in table 3.3

Fig. 3.4 'a'

XJF/46/41

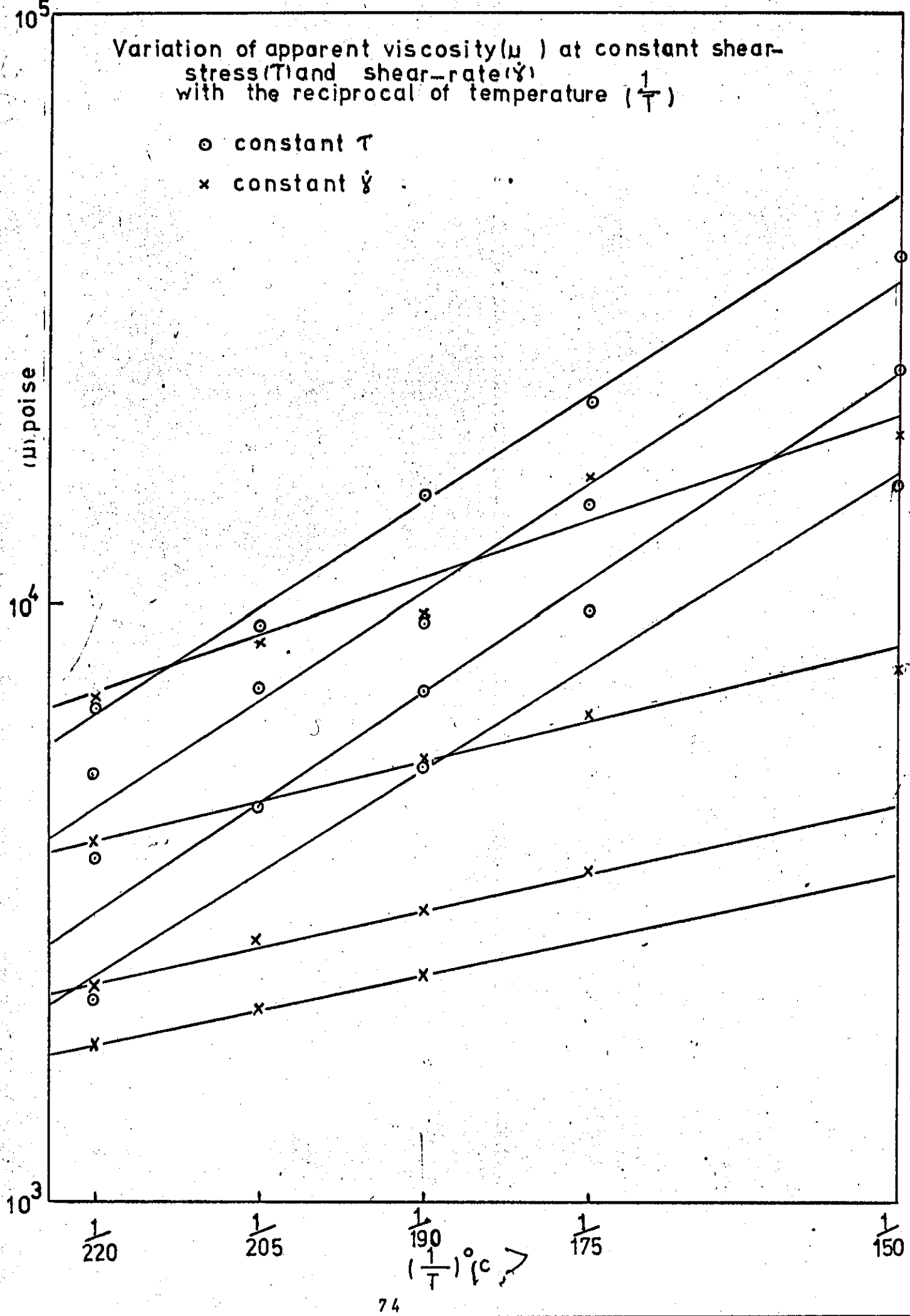

Fig. 3.4 'b'

XJF/46/63

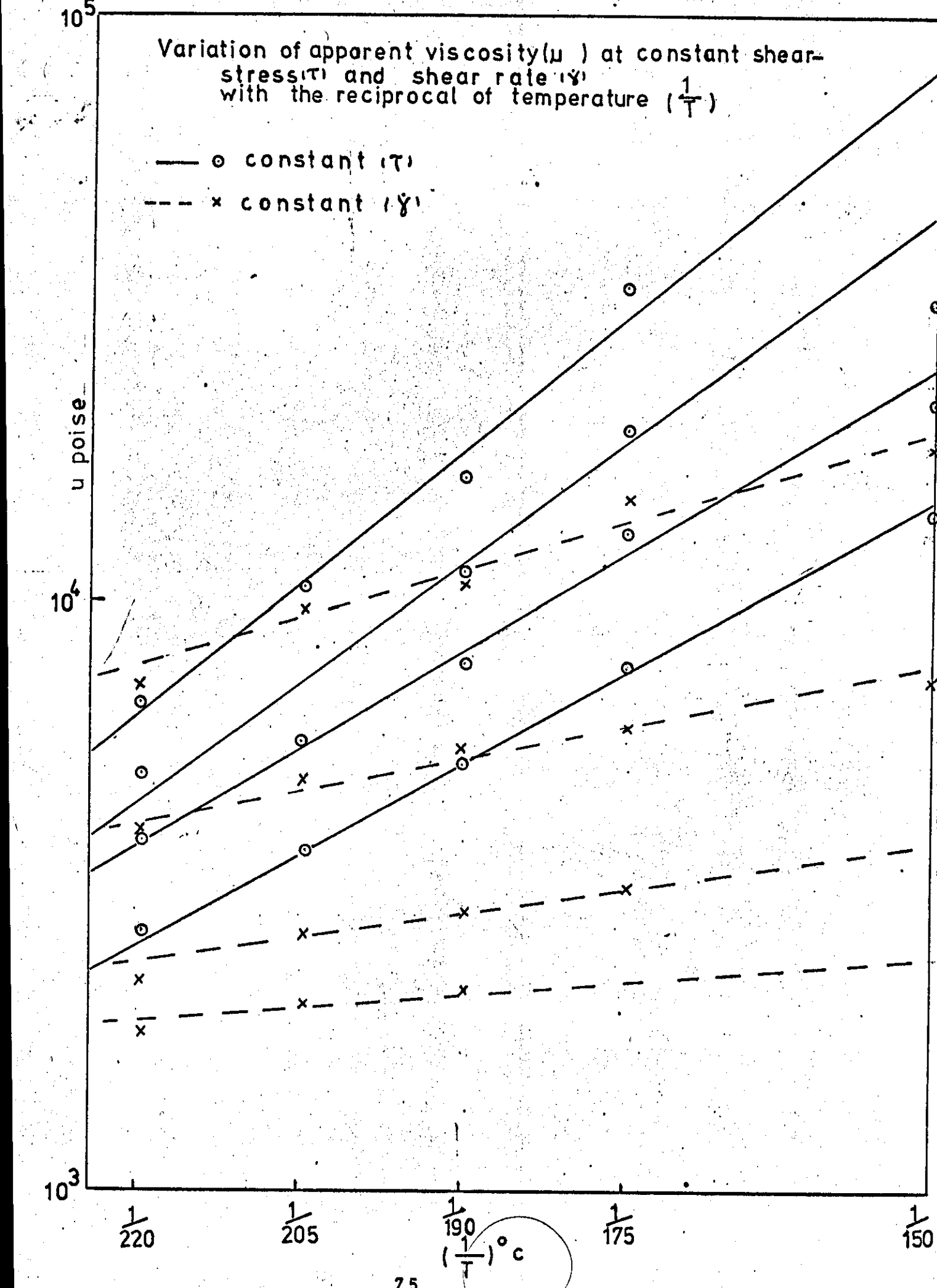

Fig. 3.4 'c'

XJF/5

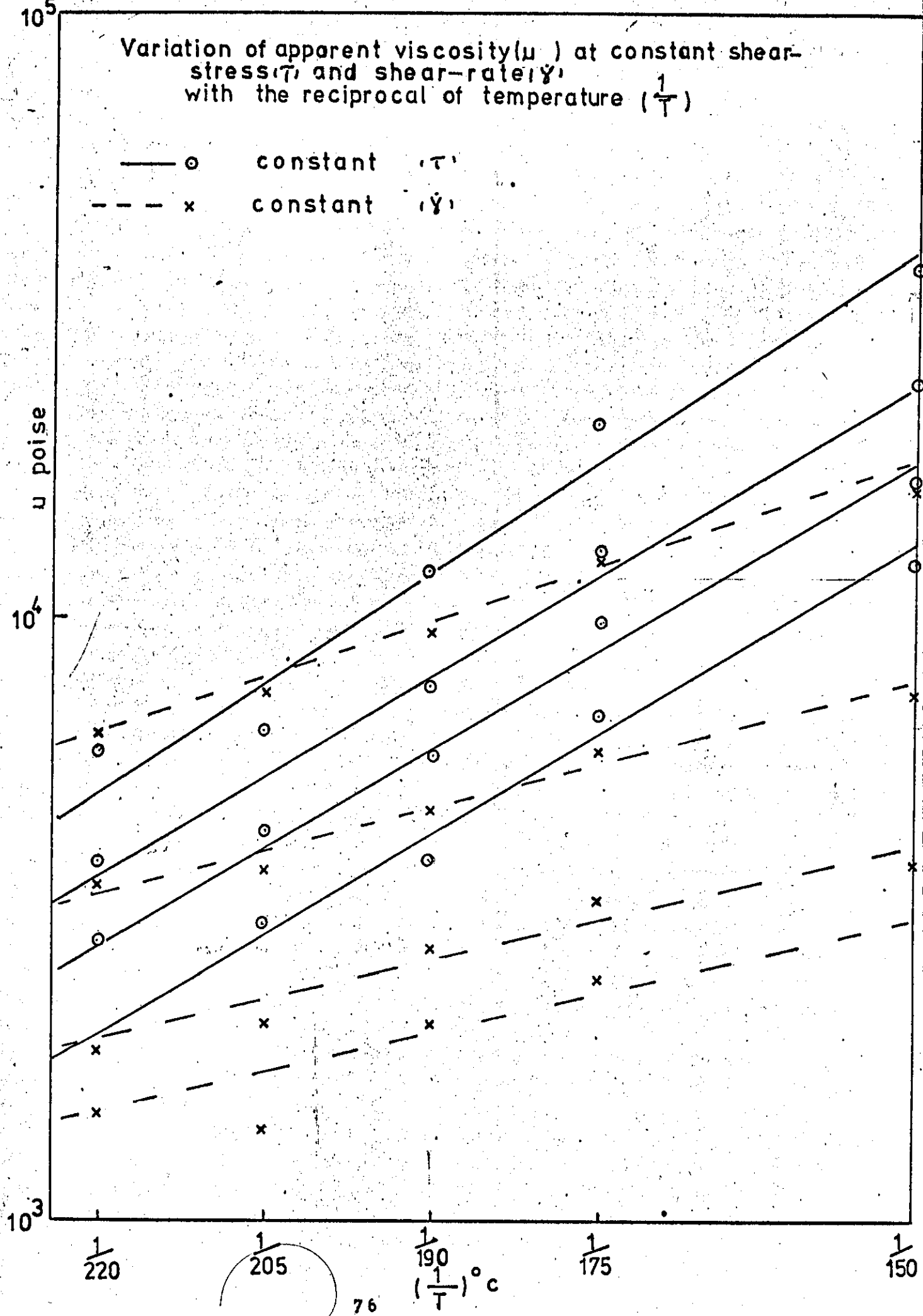
Variation of apparent viscosity(μ) at constant shear-stress(τ) and shear-rate(γ̇)
with the reciprocal of temperature (1/T)
constant (τ)
constant (γ̇)
μ poise
10^5
10^4
10^3
1/220
1/205
1/190
1/175
1/150
(1/T)°c

Fig. 3.4 'd'

XJF/25

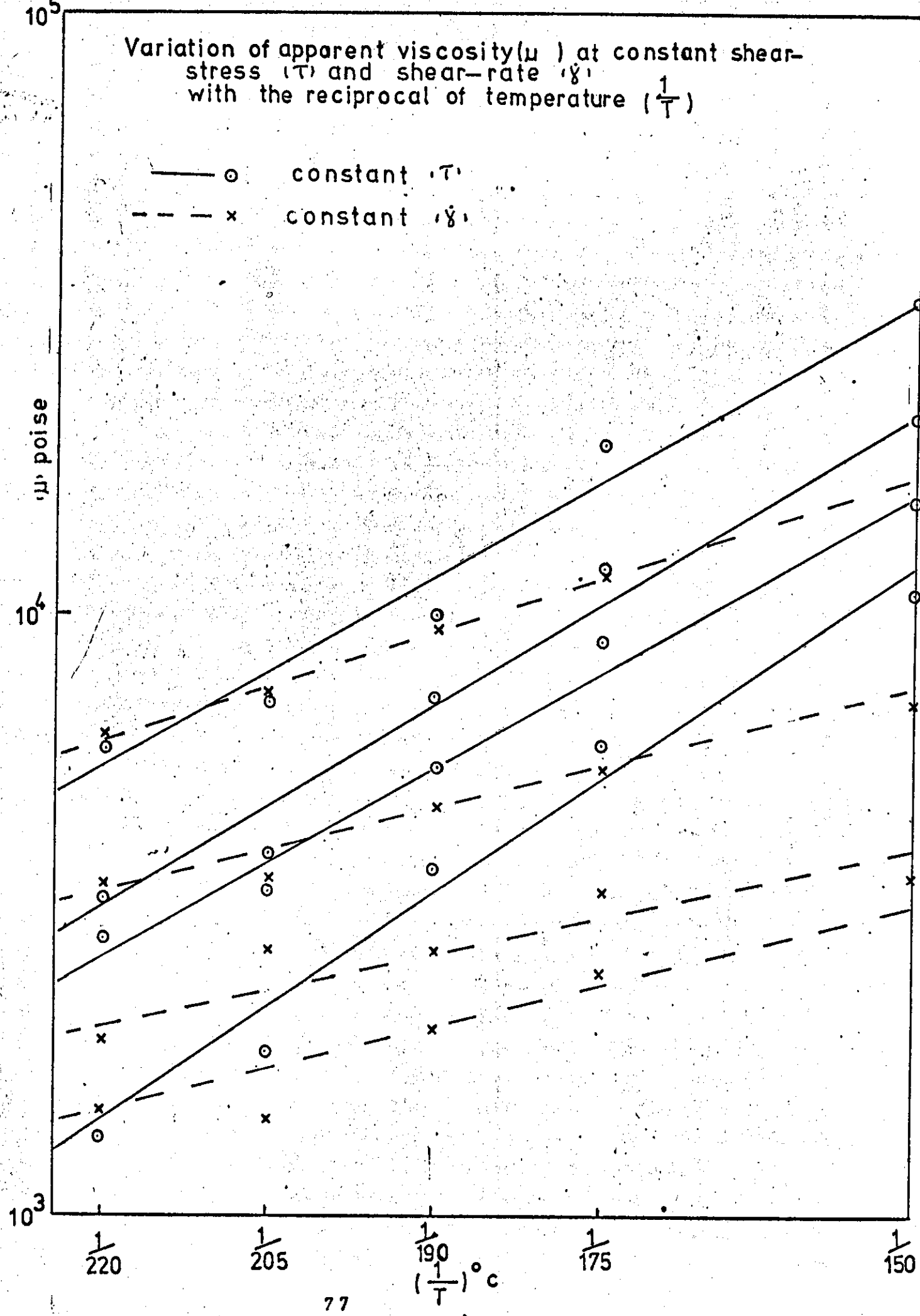

Fig. 3.4 'e'

XJF/50

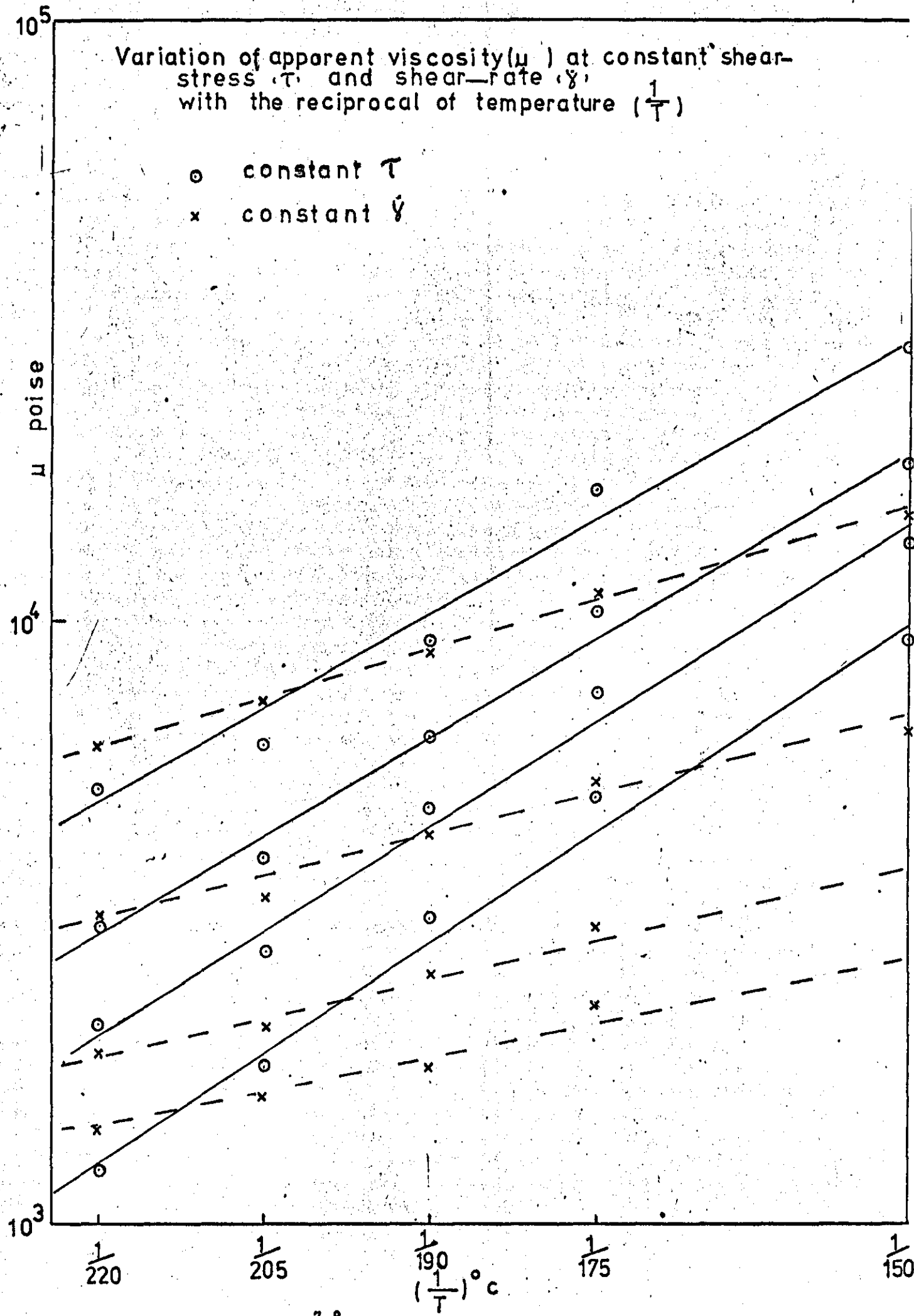

Fig. 3.4 'f'

XJF/100

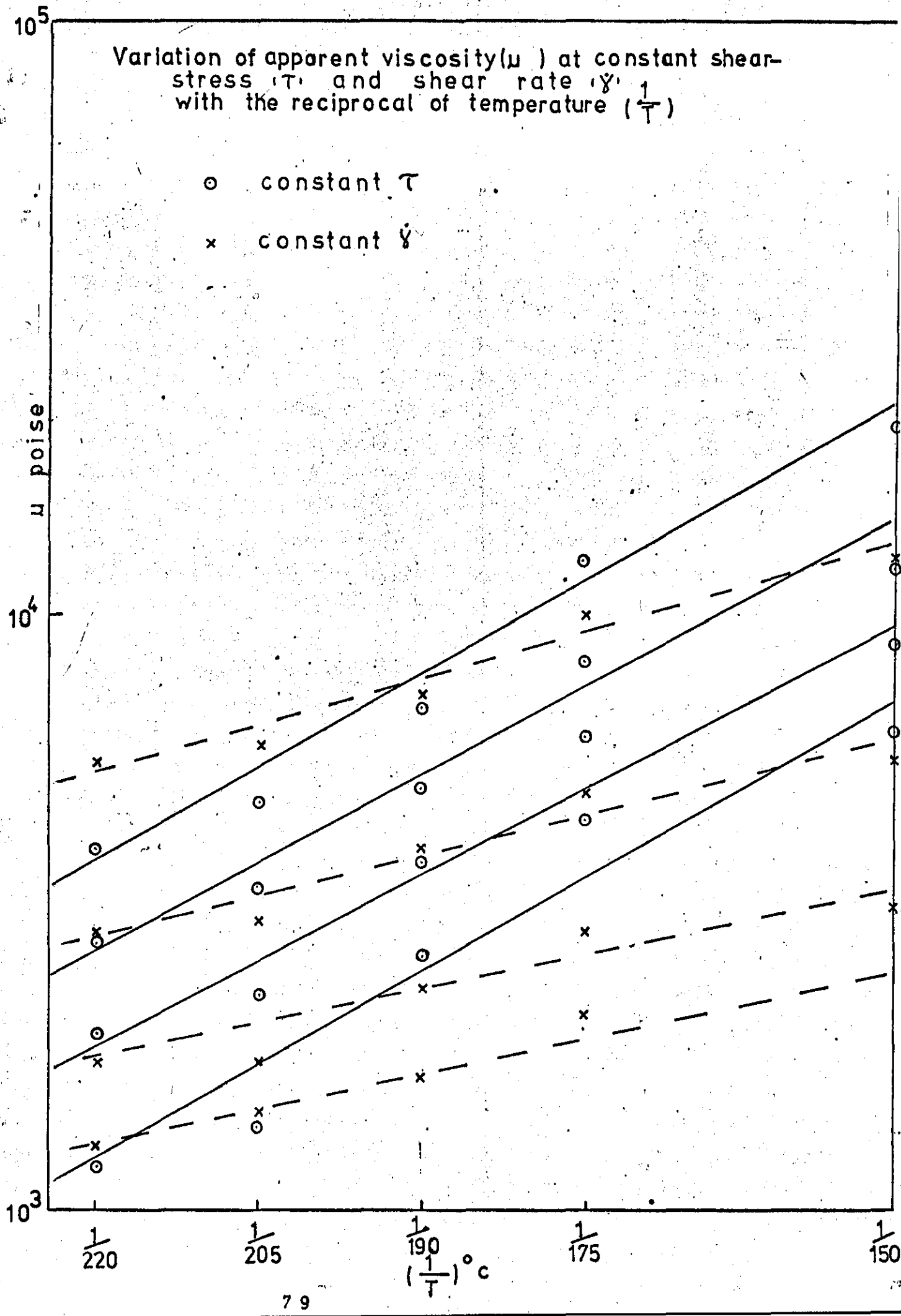

Table: 3.3 : Apparent Activation Energy (ΔE_τ) at constant shear stress (τ)

τ (p.s.i.)	ΔE_τ K cal/mole					
	XJF/5	XJF/25	XJF/50	XJF/100	XJF/46/41	XJF/46/63
5.6	12.0	10.8	10.4	10.3	12.4	14.9
9.0	11.1	11.2	11.0	10.0	12.5	14.0
12.0	10.8	10.8	11.5	10.0	12.7	12.0
16.0	10.8	12.4	12.2	10.6	12.3	12.0
	Apparent Activation Energy, $\Delta E_{\dot\gamma}$, at constant shear rate, $\dot\gamma$,					
$\dot\gamma$ sec^{-1}	$\Delta E_{\dot\gamma}$ K cal/mole					
	XJF/5	XJF/25	XJF/50	XJF/100	XJF/46/41	XJF/46/63
50	6.5	5.7	5.7	4.6	6.7	5.7
200	4.9	4.6	4.7	4.1	4.5	3.8
500	4.0	3.6	3.6	3.6	4.2	2.8
800	3.9	4.8	3.7	4.2	3.7	1.6

3.2 Effect of Extrusion Conditions on Mechanical Properties of the Low Density Polyethylene Films.

3-2.1 Haul-off Rate :

In Table 3.4 is illustrated variation of the haul-off rate with blow-up ratio and screw speed in the film-blowing process for the studied polyethylene grades.

From results it can be seen that resin MS/5 required highest draw down (highest haul-off rate) to draw to the same film thickness (60 microns) under equal conditions of screw speed and blow-up ratio, whereas resin MS/100 required the lowest haul-off rate.

This difference in the haul-off speed can be interpreted to a difference in the output rate under the same extrusion conditions. The lower the slip, the higher is the output rate. The increase in the output rate in case of the low slip grades may have resulted from two effects:

First, the low slip grade polymer, having a relatively higher friction, can be conveyed more easily along the extruder barrel. At the same time, the high friction effect of the low slip grade may result in an increase in the extrusion temperature in the barrel, an effect which may also lead to an increase in the output rate.

Table: 3.4 : Variation of haul-off rate with Blow-Up ratio and screw speed

Screw speed, R.P.M.	Blow-Up Ratio	Haul-off rate, ft./min.					
		XJF/46/41	XJF/46/63	XJF/5	XJF/25	XJF/50	XJF/100
25	0.7	25.2	20.7	28.9	25.3	24.3	22.5
	1.0	21.6	14.4	22.6	20.7	19.7	18.0
	1.4	14.4	10.8	18	16.2	14.4	13.1
	1.8	9.9	8.1	14.4	13.2	12.6	12.6
	2.1	8.1	7.2	-	-	11.7	10.8
35	0.7	32.4	28.8	38.7	36	32.4	29.7
	1.0	25.2	19.8	29.7	27	25.2	24.3
	1.4	20.7	16.2	25.2	22.5	20.7	18.0
	1.8	15.6	12.6	15.3	13.5	12.6	11.7
	2.1	12.6	10.1	10.8	9.9	9.0	9.0
	2.5	-	-	-	-	8.1	7.6
45	0.7	46.8	34.2	47	42.3	37.8	35.1
	1.0	36	30.6	34.2	32.4	30.6	28.8
	1.4	27	21.6	30.6	27	23.4	19.8
	1.8	20.6	16.2	23.4	21.6	19.8	16.2
	2.1	16.2	11.7	18.5	15.3	14.4	13.5
	2.5	12.8	9.0	11.7	9.9	9.8	9.0
	2.8	10.1	7.5	10.0	8.5	8.1	7.2

Table: 3.4 (continued)

Screw speed, r.p.m.	Blow-up Ratio	Haul-off rate, ft./min.					
		XJF/46/41	XJF/46/63	XJF/5	XJF/25	XJF/50	XJF/100
55	0.7	48.6	39.6	53.1	48.6	43.2	37.8
	1.0	41.4	32.4	46.8	43.2	36.0	30.6
	1.4	28.8	25.2	35.1	31.5	27	24.3
	1.8	23.4	17.2	30.6	25.2	22.5	19.8
	2.1	18	12.6	22.5	19.8	18.0	16.2
	2.5	16.2	10.4	19.8	18.0	14.4	13.5
	2.8	12.7	7.0	14.1	15.2	11.4	10.8

3-2.2 Effect of Blow-up Ratio :

The effect of blow-up ratio on tensile, tear and impact strengths can be seen from table 3.5 (a,b,c,d,e,f,) for film made from each grade of the six studied polyethylenes.

The variation of tensile strength in both machine and transverse directions with blow-up ratio is immediately detected from table 3.5. Data from this table have been plotted in fig. 3.5 for resin MS/5 (low slip) and resin MS/100 (high slip) over a wide range of blow-up ratio and screw speed.

For all the resins studied and at all conditions of screw speed tensile strength at break decreased in the machine direction and increased in the transverse direction with increasing blow-up ratio.

Average elongation at break as revealed by data from table 3.6 increased in the machine direction and decreased linearly in the transverse direction. In fig. 3.6 is illustrated variation of transverse elongation at break with blow-up ratio, from which it follows that transverse elongation at break is highest for the highest slip grade (resin MS/100) and decreased with degree of slip. Resin MS/5 (low slip) displayed the lowest value of transverse elongation at break.

Tear propagation increased sharply with blow-up ratio in the machine direction whereas the transverse direction tear is almost constant . Variation of tear strength in both machine and transverse directions is shown in fig. 3.7, for all studied grades.

Falling dart impact strength increased significantly with blow-up ratio for all film grades. The effect of blow-up ratio on impact strength can be seen from fig. 3.8 for film made from the two standard polyethylene grades (XJF/46/41 and XJF/46/63).

Table : 3.5 (a)

Variation of Tensile strength, tear propagation and impact strength with blow-up ratio and screw speed for film made from L.D. Polyethylene

M = Machine direction
T = Transverse direction

Film Density = 0.9206 g/cm^3

XJF/46/41

Screw speed r.p.m.	Blow-up ratio	Tensile strength MN/m^2		Tear strength, g		Impact strength g.cm
		M	T	M	T	
25	0.7	16.8	10.9	460	348	893
	1.0	17.1	12.3	440	350	1000
	1.4	16.3	11.6	445	346	1052
	1.8	16.4	14.7	390	336	1126
35	0.7	17.3	10.8	467	370	964
	1.0	17.7	12.4	452	362	1034
	1.4	16.7	15.4	403	359	1144
	1.8	15	15.0	360	349	1452
	2.1	14.6	15.1	322	330	1750
40	0.7	18.3	12.4	476	340	1070
	1.0	16.2	13.4	456	370	924
	1.4	16.0	15.9	460	356	1200
	1.8	16.0	16.2	378	340	1312
	2.1	17.6	17.9	298	330	1750
	2.5	16.8	19.0	300	301	1730
45	0.7	21.7	8.3	501	375	862
	1.0	19.6	10.4	475	360	924
	1.4	18.4	12.5	460	355	1300
	1.8	16.6	13.4	432	338	1610
	2.1	17.8	16.2	378	336	1860
	2.5	16.3	16.1	310	350	2050
	2.8	14.4	15.4	309	358	2250
55	0.7	20.3	10.2	510	366	792
	1.0	18.5	13.3	461	366	832
	1.4	15.8	14.3	470	345	924
	1.8	16.8	14.6	420	360	1563
	2.1	16.5	15.5	390	352	
	2.5	16.2	16.3	313	354	2250
	2.8	15.4	16.7	290	339	2300

Table : 3.5 (b)

Variation of Tensile strength, tear propagation and impact strength with blow-up ratio and screw speed for film made from L.D. polyethylene.

M = Machine direction
T = Transverse direction

XJF/46/63

Film Density = 0.9226 g/cm^3

Screw speed r.p.m.	Blow-up Ratio	Tensile strength MN/m^2		Tear strength, g		Impact strength g. cm.
		M	T	M	T	
25	0.7	15.8	9.6	460	352	968
	1.0	17.0	12.1	444	346	1346
	1.4	16.0	13.6	425	343	1346
	1.8	14.8	13.8	380	335	1355
35	0.7	17.9	12.0	465	342	876
	1.0	16.4	12.2	462	325	1214
	1.4	16.3	14.6	433	332	1289
	1.8	16.8	13.6	401	346	1481
	2.1	14.4	15.7	352	335	1549
40	0.7	17.0	12.3	450	323	1070
	1.0	16.5	13.2	492	332	1065
	1.4	17.1	14.8	477	341	1481
	1.8	15.5	16.1	376	354	1300
	2.1	16.1	15.4	330	350	1618
	2.5	16.0	16.3	313	348	1630
45	0.7	20	13.3	523	420	1091
	1.0	19.8	15.0	507	346	1267
	1.4	17.8	15.0	491	365	1360
	1.8	15.8	15.8	410	350	1520
	2.1	17.2	16.6	366	363	1600
	2.5	16.5	18.8	378	368	1720
	2.8	15.8	18.7	322	355	1990
55	0.7	19.2	11.3	517	375	1056
	1.0	19.4	15.1	513	365	1289
	1.4	18.3	15.8	498	370	1010
	1.8	18.1	16.5	460	363	1481
	2.1	16.5	16.7	370	356	1890
	2.5	16.3	16.5	324	358	2020
	2.8	15.1	16.9	320	363	

Table:3.5(c)

Variation of Tensile strength, tear propagation and impact strength with blow-up ratio and screw speed for film made from L-D-polyethylene.

M = Machine Direction
T = Transverse Direction

Film Density = 0.9154 g/cm^3

XJF/5

Screw speed r.p.m.	Blow-up ratio	Tensile strength MN/m^2		Tear strength g		Impact Strength g.cm.
		M	T	M	T	
20	0.7	21.4	14.4	444	340	1320
	1.0	20.2	14.7	426	341	1370
	1.4	19.0	14.6	410	336	1450
	1.8	17.0	15.7	410	333	1565
25	0.7	23.0	14.2	445	343	1370
	1.0	22.5	15.1	420	317	1396
	1.4	20.6	15.2	427	323	1480
	1.8	20.9	17.1	395	342	1590
35	0.7	25.0	14.0	453	320	1360
	1.0	25.4	12.6	460	308	1395
	1.4	21.1	17.6	455	325	1420
	1.8	19.9	17.0	350	333	1780
	2.1	19.6	18.5	340	334	2100
45	0.7	26.2	15.7	470	342	1420
	1.0	22.9	15.6	440	330	1502
	1.4	22.3	16.1	465	344	1650
	1.8	21.7	16.8	382	328	1811
	2.1	19.6	16.4	392	311	1900
	2.5	19.0	18.0	365	327	2200
	2.8	17.2	17.8	346	326	2200
55	0.7	28.0	16.4	496	360	1475
	1.0	26.0	16.8	472	334	1675
	1.4	23.8	14.1	471	350	1720
	1.8	24.1	16.9	410	351	1840
	2.1	19.2	18.4	380	324	2000
	2.5	18.6	18.6	354	327	2211
	2.8	17.2	17.2	340	340	2100

Table :3.5(d)

Variation of Tensile strength, tear propagation and impact strength with blow-up ratio and screw speed for film made from L-D-polyethylene.

M = Machine Direction
T = Transverse Direction

XJF/25

Film Density = 0.9155 g/cm^3

Screw speed r.p.m.	Blow-up ratio	Tensile strength MN/m^2		Tear strength g		Impact Strength g.cm
		M	T	M	T	
20	0.7	21.5	11.4	436	347	1316
	1.0	20.7	12.9	440	363	1355
	1.4	17.7	14.0	409	341	1440
	1.8	17.6	13.9	424	336	1535
25	0.7	21.0	12.1	432	336	1370
	1.0	21.1	12.0	437	309	1430
	1.4	19.4	16.3	422	330	1444
	1.8	18.1	16.9	402	322	1600
35	0.7	24.2	15.9	460	319	1400
	1.0	23.7	12.3	454	320	1416
	1.4	19.6	15.3	454	326	1500
	1.8	18.3	17.0	340	338	1790
	2.1	18.1	16.9	331	332	1890
45	0.7	26.6	13.6	490	340	1460
	1.0	21.3	12.7	475	341	1520
	1.4	20.4	12.6	460	356	1650
	1.8	18.8	16.9	400	348	1800
	2.1	18.6	17.5	356	350	1790
	2.5	18.0	17.8	342	339	1850
	2.8	17.5	17.9	337	330	1904
55	0.7	27.0	14.5	495	343	1513
	1.0	27.1	14.9	480	348	1700
	1.4	24.6	16.6	476	356	1770
	1.8	19.9	17.0	442	346	1841
	2.1	20.1	16.3	376	339	1842
	2.5	18.6	17.9	350	348	1870
	2.8	18.1	19.0	338	344	2200

Table : 3.5(e)

Variation of Tensile strength, tear propagation and impact strength with blow-up ratio and screw speed for film made from L-D- polyethylene.

M = Machine Direction
T = Transverse Direction

XJF/50

Film Density = 0.9157 g/cm^3

Screw speed r.p.m.	Blow-up ratio	Tensile strength MN/m^2		Tear strength, g		Impact Strength g-cm
		M	T	M	T	
20	0.7	19.1	14.1	450	340	1318
	1.0	19.0	13.9	428	344	1334
	1.4	17.6	15.2	427	340	1354
	1.8	17.9	16.3	385	339	1580
25	0.7	21.3	12.2	445	350	1350
	1.0	20.1	17.0	446	330	1410
	1.4	16.6	15.8	450	333	1590
	1.8	18.3	16.9	398	325	1630
	2.1	15.4	16.0	338	336	1690
35	0.7	21.0	13.1	470	320	1333
	1.0	24.5	14.7	460	326	1350
	1.4	19.0	16.2	464	322	1380
	1.8	17.8	17.1	376	336	1790
	2.1	18.0	16.9	330	341	1880
	2.5	17.0	17.0	320	328	2150
45	0.7	21.7	14.1	495	341	1490
	1.0	21.3	12.9	500	350	1520
	1.4	21.4	15.3	466	335	1600
	1.8	19.6	17.4	403	345	1690
	2.1	19.2	16.2	360	343	1734
	2.5	17.1	17.0	366	350	1754
	2.8	16.6	16.8	324	340	1792
55	0.7	25.8	16.8	512	338	1500
	1.0	23.0	15.3	486	352	1574
	1.4	23.6	16.1	463	350	1613
	1.8	18.5	16.7	400	342	1762
	2.1	19.1	18.4	360	335	1794
	2.5	16.7	17.9	325	355	1820
	2.8	17.0	17.7	327	350	1910

Table: 3.5 (f)

Variation of tensile strength, tear propagation and impact strength with blow-up ratio and screw speed for film made from L-D- polyethylene.

M = Machine direction
T = Transverse direction

XJF/100

Film Density = 0.9158 g/cm^3

Screw speed r.p.m.	Blow-up ratio	Tensile strength MN/m^2		Tear strength g		Impact Strength g-cm
		M	T	M	T	
20	0.7	20.2	12.2	453	345	1420
	1.0	18.6	12.8	435	350	1460
	1.4	16.8	13.4	430	349	1490
	1.8	16.6	13.3	395	352	1535
25	0.7	21.2	12.0	461	342	1430
	1.0	18.7	12.6	452	310	1493
	1.4	17.0	16.6	430	318	1500
	1.8	18.0	17.0	389	306	1560
	2.1	16.4	17.9	313	310	1660
35	0.7	24.0	15.8	464	344	1370
	1.0	24.5	11.3	489	330	1417
	1.4	19.6	17.5	470	336	1438
	1.8	17.5	17.1	351	351	1810
	2.1	18.8	17.9	328	345	1867
	2.5	17.0	16.4	301	350	1900
45	0.7	25.2	13.8	488	358	1560
	1.0	25.4	12.4	502	335	1590
	1.4	20.3	11.9	487	360	1650
	1.8	20.5	17.6	411	356	1675
	2.1	19.0	17.7	354	360	1690
	2.5	16.3	17.5	366	364	1720
	2.8	15.4	17.9	310	351	1810
55	0.7	26.3	14.6	511	373	1550
	1.0	24.0	15.2	498	361	1594
	1.4	19.8	16.0	474	364	1662
	1.8	20.4	17.2	430	358	1770
	2.1	19.0	17.0	366	350	1788
	2.5	19.0	18.0	314	360	1800
	2.8	17.6	18.6	316	365	1864

Fig. 3.5 :

Variation of tensile strength with blow ratio and screw speed.

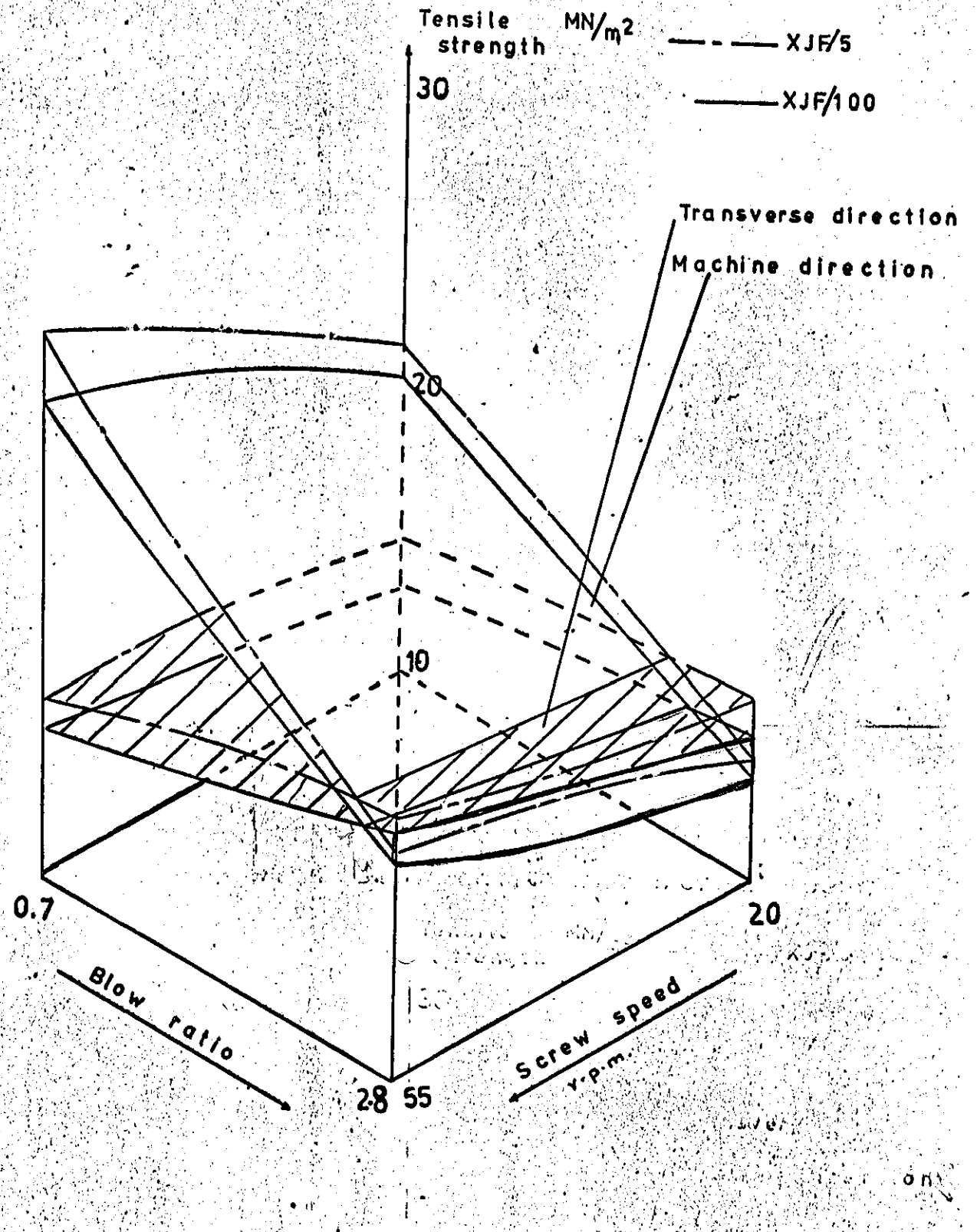

(Statistically smoothed data)

Table: 3.6 Variation of % Elongation at break with blow-up ratio and screw speed

Screw speed r.p.m.	Blow-up Ratio	% Elongation at Break							
		XJF/5		XJF/25		XJF/50		XJF/100	
		M	T	M	T	M	T	M	T
35	0.7	348	551	324	514	256	652	250	555
	1.0	376	437	333	516	295	590	282	576
	1.4	370	420	375	486	288	533	312	490
	1.8	400	349	390	410	326	486	346	476
	2.1	453	350	417	334	324	470	375	406
45	0.7	335	476	267	562	333	650	340	663
	1.0	330	444	307	560	357	588	377	637
	1.4	401	425	385	500	380	550	369	598
	1.8	426	401	406	451	399	502	370	533
	2.1	448	361	464	400	396	450	371	500
	2.5	450	313	488	317	447	367	393	410
	2.8	477	290	488	310	490	360	388	390
55	0.7	351	496	306	575	340	660	333	664
	1.0	374	455	324	557	350	600	367	640
	1.4	403	470	376	516	366	546	368	605
	1.8	417	409	355	423	375	511	380	585
	2.1	437	374	386	433	401	463	381	560
	2.5	435	320	403	360	408	374	394	516
	2.8	452	303	424	315	476	370	405	433

Fig. 3.6

Variation of transverse elongation at break (E_T) with blow ratio (B.R.)

Screw speed = 45 r.p.m.

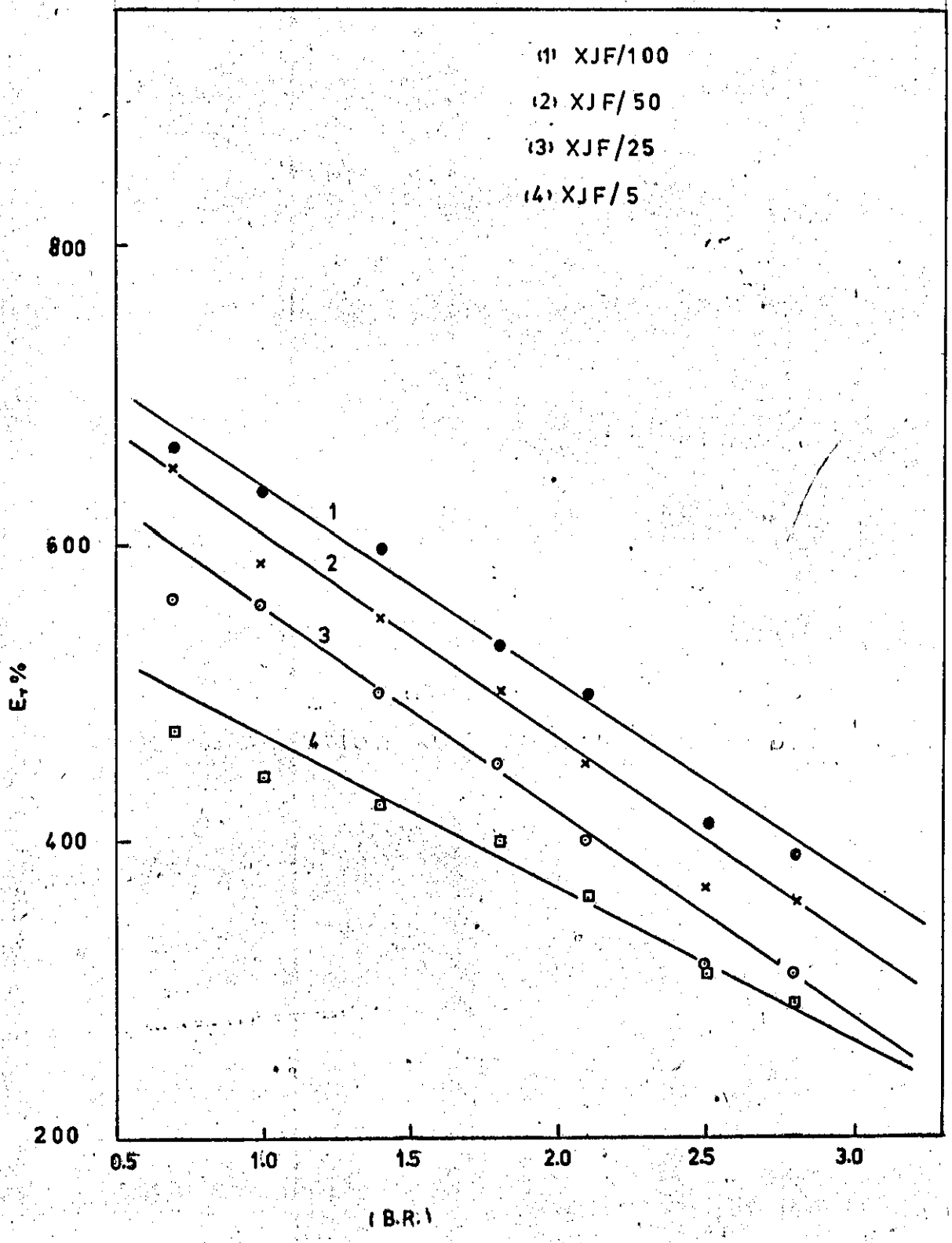

Fig. 3.7:

Variation of tear strength with blow ratio (B.U.R.). Screw speed = 45 r.p.m. (Statistically smoothed data)

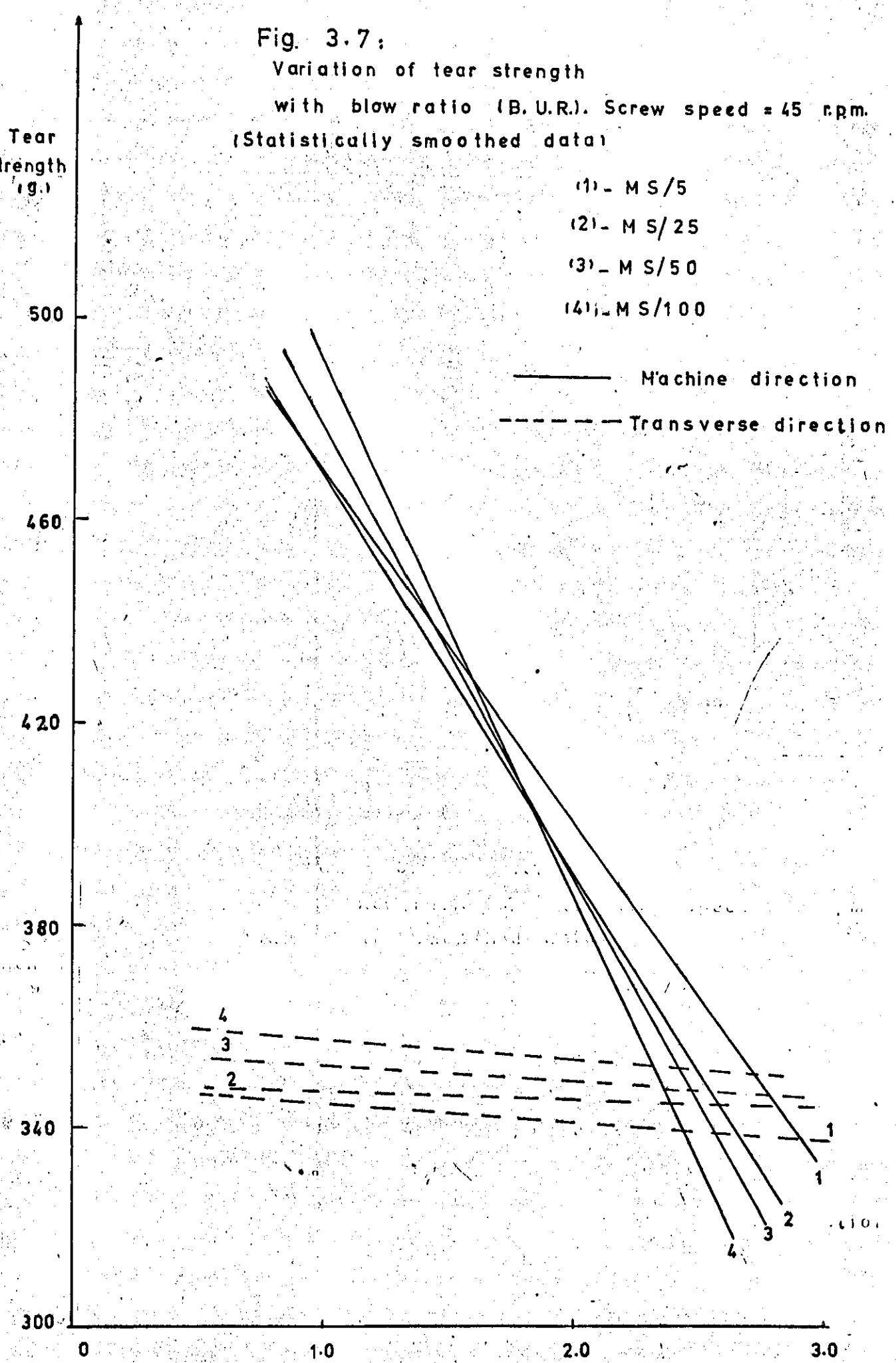

Fig.3.8 : Variation of impact strength with blow ratio.

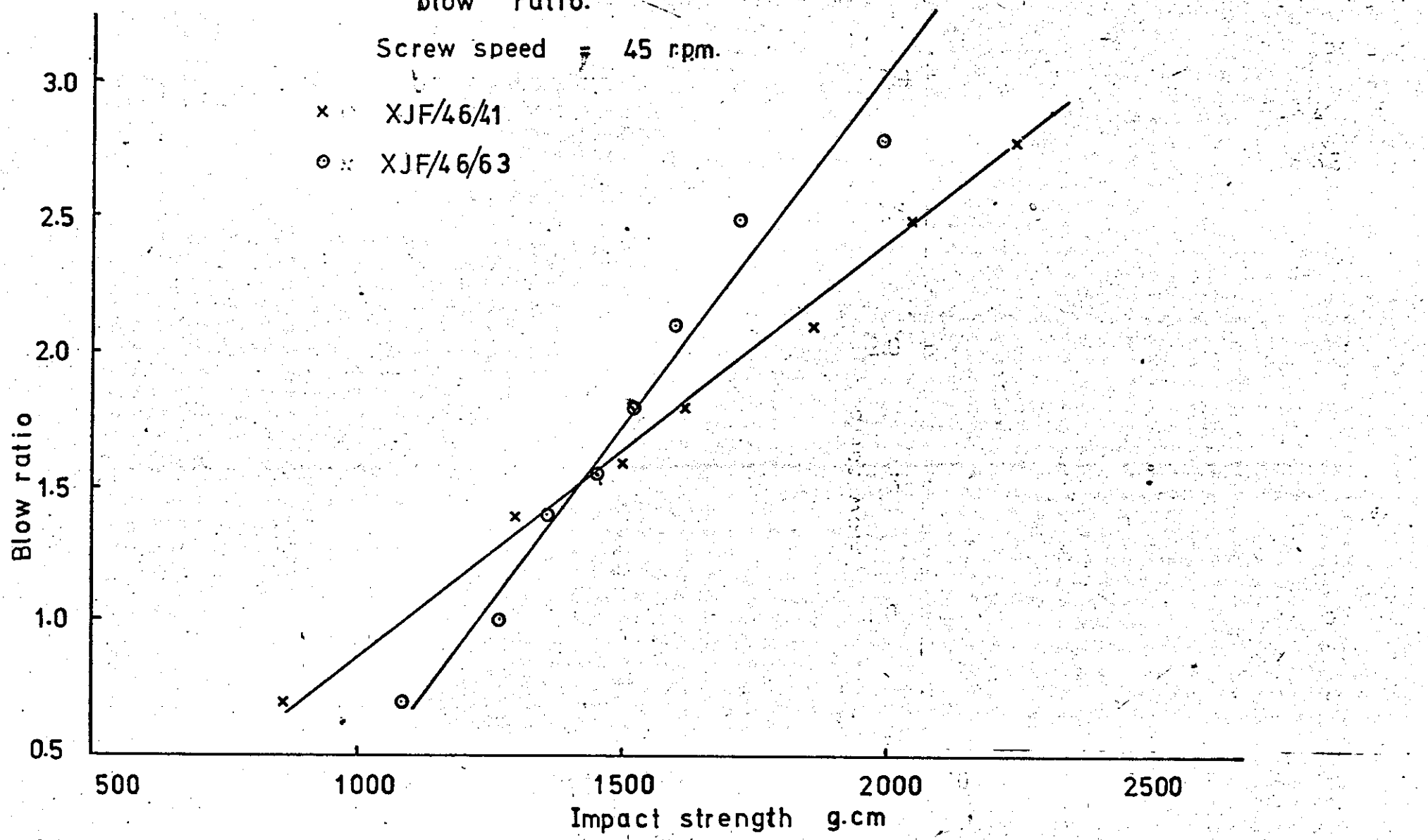

These changes in average strength properties indicated the more balanced strength properties in the film were obtained as the blow-up ratio was increased from 0.7:1 to (2.5 - 2.8) :1.

Generally, the highest values of film strength properties were found to hold for film made from the low slip grade (MS/5) at blow-up ratios between 2.4 — 2.6 .

3-2.3 Effect of Screw Speed :

A general effect of the screw speed or, output, rate, is also revealed by table 3.5. Increasing the output rate by increasing screw speed caused a significant increase in the film strength (tensile, tear and impact strength).

SECTION 4

Discussion of the Results and Conclusion

4.1 Flow of the Low Density Polyethylene grades:

The non-Newtonian flow of the different polyethylene samples and the effect of the slip agent on the flow behaviour can be interpreted in the following way:-

When a polyethylene melt is sheared inside a tube the molecules will tend to align themselves in the direction of shear. This alignment, or, orientation of the molecules, depends greatly on the shear-rate ($\dot{\gamma}$) and becomes more perfect as the shear-rate is increased. On the other hand, orientation of the molecules is opposed by the randomizing influence of Brownian motion, which tends to disrupt any aligned molecules. Therefore, relatively complete orientation is reached when the rate of orientation is great enough to offset the disrupting effect of random molecular (Brownian) motion.

Thus, where at extremely low shear rates the balance will be in favour of the disrupting Brownian forces, at extremely high shear-rates it will be in favour of the orienting forces, as the disrupting effects of Brownian motion are negligible. At extremely high shear-rates, further increases in shear-rates would have very small effect on the degree of orientation and the material would approach Newtonian behaviour.

However, due to the fact that capillary dies of considerably large diameters were not available, it was not possible to extrude the polyethylene melt at very low shear-rates, and, therefore, the expected region of Newtonian behaviour (first Newtonian region), which normally occurs at shear-rates lower than 10^{-1} sec^{-1}, does not appear in the flow curves shown in fig. 3.1. In the present work the lowest shear-rate

detected, using die No. (1) (section 2), was 16.6 sec^{-1}.

As increases in temperature would tend to increase the Brownian motion, and, therefore, make complete alignment of the molecules more difficult, it is expected that the inception of non-Newtonian behaviour would be delayed to still higher shear-rates. This explains the gradual shifting of the flow curves shown in Fig. 3.1 towards Newtonian behaviour with increases in temperature. A clear picture of the effect of temperature on the flow behaviour of the polyethylene grades may be seen from table 3.2. The degree of Newtonian behaviour, as represented by the power law exponent (n), increased significantly with temperature for all grades. The highest value of n was exhibited at 220°C at the lowest shear-rate range (10-50) sec^{-1}. This is because at this shear-rate range, the flow curves would approach the first Newtonian region, which had been delayed to still higher shear-rates by the increased temperature, i.e. the shear-rate at which non-Newtonian behaviour first began increased appreciably with increasing temperature.

As can be seen from the flow curves, the slip agent reduced the shearing stresses on the polyethylene melt and increased fluidity by providing internal lubrication for the polymer molecules. As a result of that a decrease in the melt viscosity was obtained (Fig. 3.2). The less non-Newtonian behaviour exhibited by the high slip gradesat high temperatures (205, 220°C) and high shear-rates may be interpreted by the fact that the high slip grades, due to their relatively higher fluidity, experience higher orientation of the molecules inside the tube compared to the relatively less oriented molecules of the low slip grades, which are unable to slide as readily past one another. This difference in orientation will provide some extra degree of opposition to the Brownian

disrupting motion, and, therefore, will reduce the degree of non-Newtonian behaviour and tend to bring earlier the second Newtonian region, which normally occurs at extremely high shear-rates (over 1000 sec^{-1}).

It was not possible, however to obtain viscometric data at extremely high shear-rates, as the inordinately high shear-stresses in the polymer melt, flowing at high shear-rates, caused mechanical break down, or, fracture of the extrudate. This can be seen from table 3.1 and fig. 3.3, from which it follows that an increase in temperature leads to an apparent improvement in processability as indicated by an increase in critical shear-rate.

It is pertinent to note that the critical shear-rates (table 3.1) below which smooth melt is extruded, correlate with the data presented in the same table, illustrating the shear-rate dependence of the apparent melt viscosities. The resins with the higher melt viscosities are the most susceptible to fracture at all temperature ranges. This coincides with Howell's and Benbow's findings that critical shear-stresses and shear-rates of polymer melts may depend on the melt viscosities.

4.2 ACTIVATION ENERGY

Generally, in the flow of a polymer melt under a stress gradient, the molecules in one equilibrium position surmount an energy barrier and get into new positions, causing the liquid to flow. The change in rate of flow with temperature is given by the Arrhenius equation (equation 11). As temperature falls the polymer melt flows more slowly because fewer molecules have sufficient energy to surmount the energy barrier and move to more stable positions.

From results, illustrated in table 3.3, it can be seen that the apparent viscosities at constant shear-stress may be adequately fitted to Arrhenius equation over the temperature range covered, but that such an equation does not adequately represent the constant shear-rate data over this temperature range. Results also show that apparent activation energies for viscous flow of the polyethylenes at fixed shear-rates ($\Delta E_{\dot{\gamma}}$) decrease as the level of shear-rate increases. Apparent activation energies at fixed shear-stresses (ΔE_{τ}) are independent of shear-stress. As can be seen from table 3.3 the variations of ΔE with τ are small and without a trend.

The results above are in agreement with the mathematical conclusion of Bestul and Belcher that ΔE_{τ} should at all times be greater than $\Delta E_{\dot{\gamma}}$. Their experimental results for several polymers, not including polyethylene, showed ΔE_{τ} to be roughly constant with changing shear-stress.

Philippoff and Gaskins reported a significant increase in ΔE_{τ} from 12.8 to 19 Kcal/mole over the shear-stress range ($0-16^6$) dynes/cm^2 for low density polyethylene. Whereas Schott and Kaghan reported ΔE_{τ} to be relatively constant with changing shear-stress for low

density polyethylene and to have a value of approximately 12 Kcal/mole. The present work, thus, provides confirmation of Kagan and Schott's findings that ΔE_τ is relatively constant with changing τ for all studied grades. The values of the activation energies exhibited by the different sample grades were almost the same and, therefore, in the present work, activation energies can not be employed as a processability criteria.

4.3 The Extrusion Process of Low Density Polyethylene Film

4.3.1 Orientation of Blown Film

The variation in the mechanical properties (tensile, tear and impact strengths) between the different polyethylene films can be discussed in terms of orientation of the film, which occurs as a result of the alignment of the polymer molecules. When stress is applied to a molecule of the polymer, it will take up a non-random configuration, but when the stress is removed, the molecular movements will cause the molecule to coil-up again, or, relax. During the extrusion process, orientation of the polymer molecules occurs, which increases with increase of shear-rate. However, after the melt emerges from the die, the shearing forces are released and the molecule will start to recoil. As the melt starts to cool at this stage, the molecules will not have enough time to recoil-up and they may solidify first. The amount of frozen-in orientation depends on the following factors:

a) Amount of initial orientation, which depends on shear-rate, and the amount of stretching the melt after it emerges from the die.

b) The average relaxation time of the melt.

c) The time taken by the melt to cool from the processing temperature to the solidifying temperature.

The first stage of orientation occurs in the die due to the shearing of the viscoelastic melt, which produces orientation in the machine direction (vertically upwards). After the extrusion through the anhular die, both the forward stretching and the sideways blow-up occurs in the melt before the polymer crystallizes at the freeze-line.

The forward stretching takes place first and produces some orientation of the molecules in the viscous melt parallel to the machine direction. This orientation is subsequently reduced by the blow-up process, which produces a transverse orientation as a result of blowing-up the bubble after it leavesthe die. Since the cooling of the polyethylene melt allows molecular relaxation to occur up to the point at which it solidifies (freeze-line), the orientation occuring immediately before the freeze-line is most important, since there is no further chance for relaxation to occur. Thus, in the film blowing process, only molecules that have been oriented just before the melt freezes will remain in the oriented state. Because of this, the order in which drawing down and transverse stretching of the film occurs will affect its mechanical properties. (In the light of the above, the results are discussed and correlated with the flow properties of the different samples as follows.)

4.3.2 Effect of Rheological Properties on the Mechanical Properties of the Film

Differences in draw-down can have an effect on film mechanical properties. Draw-down speed depended on the output rate for the material, the high slip grades (XJF/46163 and MS/100) requiring less take-up speed to obtain the same film thickness than the low slip grades (table 3.4).

If the freeze-line is low such that this machine direction orientation is retained in the film, then the greater unbalance between the machine direction and transverse direction orientations will lead to a film with a tendency to split in the machine direction, and will thus exhibit a low impact strength and low transverse direction tensile strength. This behaviour occurred when low blow-up ratios were employed (table 3.5).

Of particular interest is the behaviour of the curves showing variation of impact strength with blow-up ratio for films made from resins XJF/46/41 and XJF/46/63 in fig. 3.8, and resins MS/5 and MS/100 in fig. 4.1. The impact strengths of the relatively low slip grades XJF/46/41 and MS/5 increased more significantly than for the high slip grades XJF/46/63 and MS/100. At low blow-up ratios, the high slip grades exhibited higher values of impact strength, up to a blow-up ratio near 1.4-1.5, after which impact strength values were higher for the low slip grades, increasing significantly with blow-up ratio.

This behaviour could be interpreted to the fact that at low blow-up ratios the unbalance between machine and transverse direction orientation is greater for the low slip grades, which are, therefore, expected to exhibit lower values of impact strength than the high slip grades. The relatively more viscous low slip grades have greater tendency to draw

Fig 4.1 : variation of impact strength with blow ratio and screw speed.

(Statistically smoothed data)

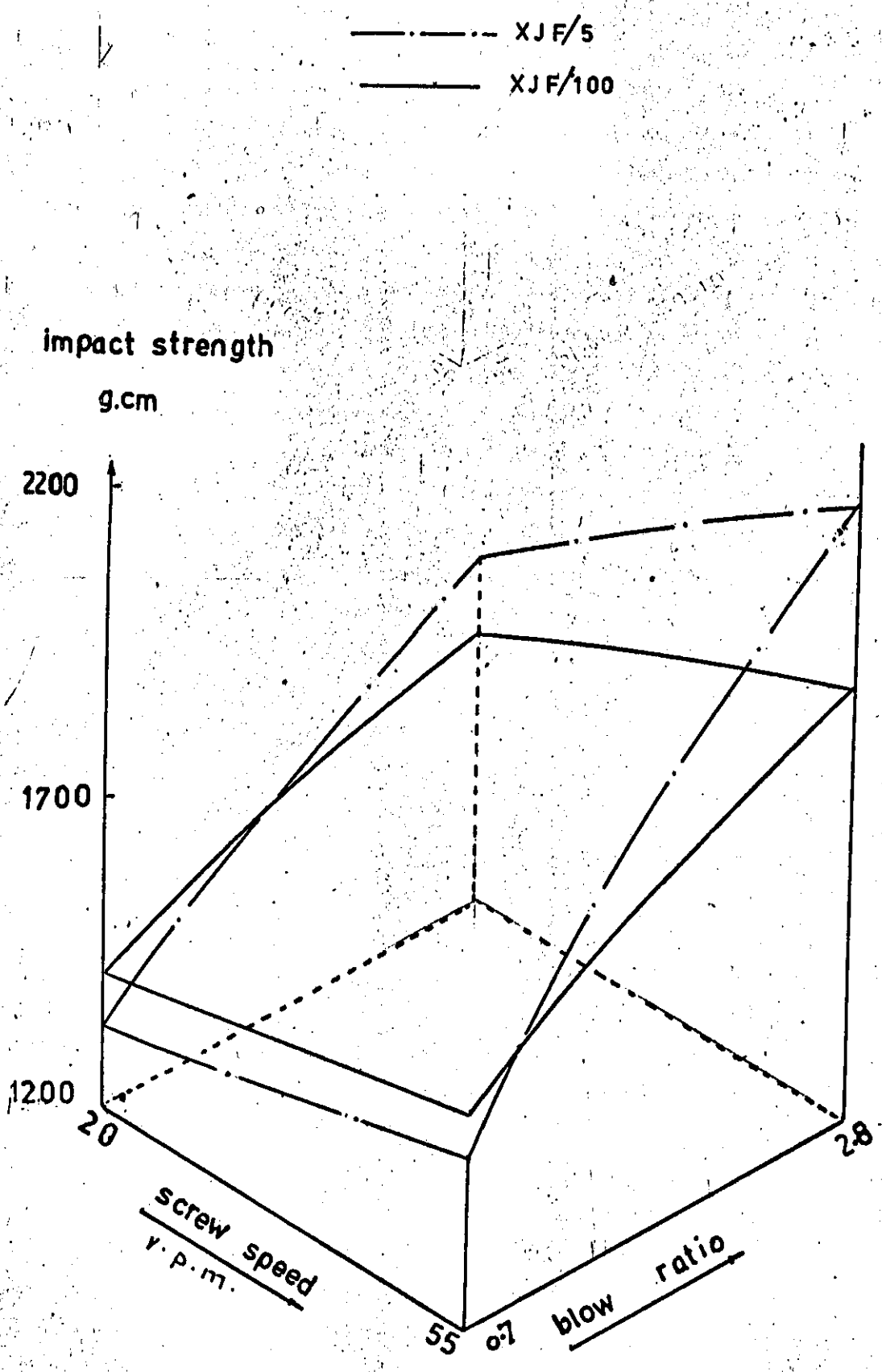

and orient over a greater part of the distance between die and freeze-line. In addition to that the low slip grades, having a relatively higher resistance to relaxation of induced orientation, can significantly retain higher degree of this orientation up to the freeze-line. The high slip grades tend to draw abruptly to their ultimate thickness building-in less significant orientation.

It was quite noticable that extruding the low slip grades at low blow-up ratios, (0.7-1) :1, was a very difficult process due to the fact that the film often fractured. This can be interpreted to the high predominancy of machine direction drawing over the transverse drawing, which resulted in a very weak transverse direction orientation and subsequent fracture of the bubble along the machine direction.

Although rheological properties of low density polyethylene were shown to have major effects on film impact strength, some authors reported that the degree of crystallinity, which can be found from density measurements, of the polyethylene, and more particularly, of the finished film, also may have significant influence on this property.

However, the densities of the films produced from the four sample grades wereshown to have very similar values (table 3.5).

4.3.3 Effect of Extrusion Conditions

(i) Tensile and Impact Strengths

The machine direction increase and transverse direction decrease of the tensile strength with blow-up ratio indicates that as the blow-up ratio is increased, the transverse direction drawing tends to build-up a transverse orientation at the expense of that in the machine direction. This orientation, however, becomes more balanced at higher blow-up ratios (2.5 - 2.8).

As the output rate is increased by increasing the screw speed, orientation will also increase as a result of the consequent increase of the haul-off rate (draw-down) to obtain the desired film thickness. This explains the significant increase in the machine direction tensile and tear strengths and the increase in impact strength which resulted from increasing screw speed (table 3.5).

The effects of orientation on impact strength are what might be expected from tensile behaviour. Impact failure occurred in the direction having the lower tensile strength and resulted in a split in the film parallel to the direction of higher tensile strength.

(ii) Elongation-Tear Relationship

From data in table 3.5 and 3.6, a correspondence may be drawn between the transverse direction elongation and the machine direction tear strength, and the machine direction elongation and the transverse direction tear strength. It is quite generally accepted that ultimate properties such as tensile strength and elongations are largely determined by the presence of flaws or defects in the materials. Failure occurs by the propagation

of cracks originating from such flaws in a direction perpendicular to the tensile force. Thus, one can rationalize the elongation values as well as the tensile strength by simply referring to the explanation for tear strength which determines the propagation of cracks or flaws. Thus, the transverse direction elongation is high because the tear strength in the machine direction is high and machine direction cracks propagate with difficulty. This relation is again noticable from variation of blow-up ratio with tear strength. Increasing blow-up ratio resulted in a decrease in the machine direction tear strength (fig. 3.7) as well as a decrease in the transverse direction elongation (fig. 3.6). Transverse direction tear strength remained nearly constant with increasing blow-up ratio while machine direction elongation increased only very slightly.

As impact strength is less affected by flaws, it continued to rise with increase of blow-up ratio.

4.3.4 Conditions of Balanced Film

From data presented in table 3.5 the conclusion may be drawn that, in order to produce a film with high mechanical properties, a high and balanced orientation in the machine and transverse directions is desirable. The use of high blow-up ratios to obtain film with more balanced orientation leads to increased impact strength, balanced tensile strength in both machine and transverse directions and a decrease in the machine direction tear strength. A compromise, must, therefore, be obtained between these properties.

In the present studied samples a balanced film was obtained at blow-up ratios between (2.4-2.8) : 1. Table 3.7 below illustrates tensile, tear and impact strength properties of balanced film for the highslip grade

(MS/100) and the low slip(MS/5) at a screw speed 55 r.p.m. and blow-up ratio ranging between (2.4-2.6) : 1 to obtain film thickness of 0.060mm.

Table 3.7:

Polymer	Haul-off Rate ft./min	Tensile Strength MN/m^2	Tear Propagation g.	Impact Strength g.cm
MS/100	13.5	18.2	340	650
MS/5	19.8	19.2	358	930

From the above table it can be seen that resin MS/5, exhibited higher film strength properties than resin MS/100, but a higher haul-off rate was required to maintain the same film thickness.

This difference in strength properties is mainly due to the higher degree of the average orientation in case of resin MS/5, which has been imposed by the relatively higher haul-off rate (fig. 3.4).

4.3.5 Birefringence

Table 3.8 illustrates variation of the birefringence with blow-up ratio from which it is seen that, generally, at low blow-up ratios all film grades exhibited high values of birefringence, which decreased significantly with blow-up ratio. The high birefringence values indicate high difference (anisotropy) between machine direction and transverse

Table: 3·8,
Variation of Birefringence, Δn, with blow-up ratio (B.U.R.)

Screw Speed	B.U.R.	$\Delta n \times 10^{-3}$			
		XJF/5	XJF/25	XJF/50	XJF/100
25	1.0	1.10	1.84	0.92	1.21
	1.8	0.71	0.54	1.30	1.09
	2.1	1.0	0.94	0.84	0.89
	2.5	0.16	0.85	0.73	0.34
35	1.0	2.21	1.90	1.00	1.76
	1.8	1.01	1.07	1.15	1.55
	2.1	1.42	1.20	1.25	0.95
	2.5	0.90	0.72	0.96	0.41
	2.8	1.13	0.93	0.57	0.61
45	1.0	2.13	2.31	2.0	1.95
	1.8	2.21	2.52	0.97	1.83
	2.1	0.90	1.90	1.52	0.81
	2.5	0.74	0.42	0.47	1.30
	2.8	0.91	0.63	0.49	0.72
55	1.0	2.70	2.42	2.51	2.00
	1.8	1.90	2.01	2.28	2.08
	2.1	1.32	1.63	1.56	1.65
	2.5	1.23	0.64	0.75	0.92
	2.8	0.75	0.91	0.66	0.65

direction orientations.

This is in very good agreement with the high machine direction tensile strength (table 3.5) exhibited at low blow-up ratios. With increasing of blow-up ratio more transverse direction orientation starts to build-up at the expense of the machine direction orientation, and it is, thus, reasonable to expect a decrease in the birefringence with increasing blow-up ratio.

The small values of the birefringence indicate that the 'balance film' condition was nearly achieved at blow-up ratios between (2.5 - 2.8) : 1.

It is pertinent to note that the highest values of the birefringence were generally, exhibited by the low slip grade (MS/5), and the lowest values were, more or less, exhibited by the high slip grade (MS/100). This ordering is substantiated with the haul-off rate values in table 3.4.

The highest haul-off rate was exhibited by resin MS/5 and the lowest by resin MS/100.

Thus, summarizing the experimental data, one can say that the molecular orientation in tubular film confirmed by the measurement of birefringence, is almost proportional to the haul-off rate, in spite of the fact that the proportional factor depends on the type of polymer and other film forming conditions.

4.4 Conclusions

The following conclusions can be drawn from the above discussions:

Application of melt rheometry helps in the assessment of low density polyethylene processability into blown film, from a knowledge of the apparent melt viscosity and the critical shear-rate. The non-Newtonian behaviour can be evaluated in terms of the power law exponent(n).

Over the entire range of temperatures covered an Arrhenius viscosity-temperature dependence equation was found to give more adequate fit for constant shear-stress data than for constant shear-rate data.

The addition of an olemide slip agent (ArO) to low density polyethylene (film grade) significantly affected two rheological properties: (a) Critical shear-rate and (b) apparent melt viscosity. While the critical shear-rate is increased by the addition of the slip agent, the apparent melt viscosity is reduced. This reduction of the apparent melt viscosity is more significant for temperatures less than 190^{o}C.

For investigations of melt flow properties, by extrusion rheometry, a method has been used to correct for entry and exit effects in capillary tube. This method proved to be reliable.

Low density polyethylene grades having different melt viscosities willhave different mechanical properties of the end films

produced. This variation is mainly imposed by the difference in haul-off rate, especially when the film is processed at low transverse orientation ratios (blow-up ratios). The relatively more viscous polymer can lead to a lower impact strength under these conditions.

In all the samples investigated over the range of blow-up ratios studied the following conclusion can be drawn.

(i) Strength properties such as ultimate tensile strength and elongation become more balanced in the machine and transverse directions as blow-up ratio is increased.

(ii) Dart drop impact strength of blown film increases as blow-up ratio is increased.

(iii) Increasing screw speed, generally, increases strength properties of the film.

(iv) From the standpoint of producing the best all-round film properties, a range of blow-up ratio from 2.5 to 2.8 was found most suitable.

(v) In general, when high haul-off rate is imposed by a certain polymer grade in the production of layflat blown film, low blow-up ratios may not be suitable. The use of dies with smaller diameters may, thus, be necessary to produce film of better strength properties.

NOMENCLATURE :

F	Force
A	Area
τ	Shear-stress
U	Velocity of fluid
μ	Apparent melt viscosity
$\frac{du}{dr}$	Velocity gradient
dt	Time
$\dot{\gamma}$	Shear-rate
K	consistency
n	Degree of non-Newtonian behaviour
η_o	Standard state viscosity
$\dot{\gamma}_o$	Standard shear-rate
R_o	Universal Gas Constant
A	Constant (frequency term)
ΔE	Energy of activation for viscous flow
Q	Output
ΔP	Pressure difference
R	Radius of tube
L	Length of tube
τ_w	Shear-stress at the wall of the tube
l_1, l_2	Lengths of one pair of die
r	Radius of one pair of die
P_1, P_2	Pressure on each die respectively
B.U.R.	Blow-up ratio
E_1	Instantaneous elastic deformation
E_2	Molecular alignment deformation
E_3	Viscous flow
$\Delta\Pi$	Birefringence
x	Piston speed
L/D	Length to diameter ratio
Gmax	Breaking Load

NOMENCLATURE contd...

Ao	Original cross sectional area
E	Elongatinn at break
Δl	Elongation at the moment of rupture of specimen
lo	Initial gauge length of the specimen
H	Height of fall of dart
W	Mass
m	Number of blows in trial run
σ_{m+1}	Impact energy of first blow of the testing run
σ_{m+2}	Impact energy of the 2nd blow of the testing run
σ_{m+20}	Impact energy of the 20th blow of the testing run

REFERENCES

Person	Mechanical Principles of Polymer Processing 1966.
Clegg P.L.	Trans. Plast. Inst. 1958.
M.J. Hughes & M.J. Cawkwell	Plastics, March 1966
A.L. Griff	Plastics Extrusion Technology 1968.
Sweeting	The Science and Technology of Polymer Films. Vol. 1 1968.
P.L. Clegg & N.D. Huck	Plastics (London) 1961.
J.R. Van Wazer Et. Al	Viscosity and Flow Measurement, Interscience 1963
N. Nakajima and M. Shida	Trans. soc. of Rheology (1966).
C.D. Han, T.C. Yu & K.W. Kim	J. Appl. Poly. Sci. 1971
C.D. Han, R.R. Lamonte	Poly. Eng. & Sci. 1971
J.P. Tordella	J. Appl. Phys. 27, 1956
P.L. Clegg, S. Turner & P.I. Vincent	Plastics 24, 31 1959
R.M. Supnik & C.M. Adams	Plast. Tech. 2, 1956
D.R. Holmes and R.P. Palmer	J. Poly. Sci., 21, 1958
M. Shida & L.V. Canico	Poly. Eng. & Sci. 11, 1971
Williamson D.A.	Packaging (Oct./Nov.) 1966
Ernest C. Bernhardt	Processing of Thermoplastic Materials 1958
J.A. Brydson	Flow Prop. of Polymer Melts 1970
J.A. Brydson	Plastics Materials 1969

Ferdinand Rodriguez	Principles of Polymer Systems 1969
British Standards Institution	Methods of Testing Plastics BS.2782 1970
American Soc. for Testing and Materials	Annual Book of ASTM Standards 1972
J.M. McKelvey	Polymer Processing 1962
J.P. Goslin & R.M. Bonner	Extrusion, Modern Plastics Encyclopedia 1965